

1 **Title**

2 **Impacts of climate change on geographical distributions of invasive ascidians**

3

4 **Running title**

5 **Climate change impacts ascidian distributions**

6

7 **Authors**

8 Zhixin Zhang¹, César Capinha², Dirk N. Karger³, Xavier Turon⁴, Hugh J. MacIsaac^{5,6}, Aibin Zhan^{7,8}

9

10 **Affiliation and address**

11 ¹ Graduate School of Marine Science and Technology, Tokyo University of Marine Science and
12 Technology, Konan, Minato, Tokyo 108-8477, Japan.

13 ² Centro de Estudos Geográficos, Instituto de Geografia e Ordenamento do Território - IGOT,
14 Universidade de Lisboa, Rua Branca Edmée Marques, 1600-276 Lisboa, Portugal.

15 ³ Swiss Federal Research Institute WSL, 8903 Birmensdorf, Switzerland.

16 ⁴ Centre for Advanced Studies of Blanes (CEAB, CSIC), Blanes, Catalonia, Spain.

17 ⁵ School of Ecology and Environmental Science, Yunnan University, Kunming, China.

18 ⁶ Great Lakes Institute for Environmental Research, University of Windsor, Windsor, Ontario,
19 Canada.

20 ⁷ Research Center for Eco-Environmental Sciences, Chinese Academy of Sciences, Beijing, China.

21 ⁸ University of Chinese Academy of Sciences, Chinese Academy of Sciences, Beijing, China.

22

23 **Corresponding author:** Prof. Aibin Zhan; e-mail: zhanaibin@hotmail.com or azhan@rcees.ac.cn.

25 **Abstract**

26 Ocean warming derived from global climate change renders marine ecosystems susceptible to
27 biological invasions. Here, we projected habitat suitability of eight highly invasive ascidians under
28 present-day and future climate scenarios. The mean sea surface temperature was predicted as the
29 most important environmental factor affecting distributions. SDM projection results indicated that
30 the tested ascidians might respond differently to future climate change. Alarmingly, the currently
31 colonized areas are much smaller than predicted. So far, a lower number of invasive ascidians have
32 been detected in some areas such as South American coasts. Such findings suggest that these
33 aforementioned areas have a high risk of new invasions. In contrast, African coasts, excluding the
34 Mediterranean side, are not prone to new invasions. Our results highlight the importance of impacts
35 of climate change on future invasions and the need for accurate modelling of invasion risks, which
36 can be used as a guide to develop management strategies.

37

38 **Keywords**

39 benthos; biological invasion; climate change; habitat; management strategy; species distribution
40 model.

42 **1 INTRODUCTION**

43 Biological invasions have been recognized as one of the most serious threats to global biodiversity
44 and have resulted in substantial ecological changes, health effects, and economic impacts (Pimentel et
45 al., 2005; Ehrenfeld, 2010; Simberloff et al., 2013; Scheele et al., 2019). Invasive species can
46 negatively impact native communities through competition and predation (Ehrenfeld, 2010;
47 Simberloff et al., 2013; Zhan et al., 2015). In addition, they are capable of transmitting parasites and
48 pathogens that cause fatal diseases and declines of native species (e.g., Kozubíková et al., 2009;
49 Scheele et al., 2019). Marine ecosystems are extremely susceptible to biological invasions owing to
50 several factors, notably intensive human activities such as global shipping and both direct and
51 indirect effects of climate changes (Stachowicz et al., 2002; Molnar et al., 2008; Olenin et al., 2011).
52 Approximately 90% of global trade relies on ships, transferring organisms *via* biofouling and ballast
53 water among coastal waters (Molnar et al., 2008; Kaluza et al., 2010; Goldsmit et al., 2018).
54 Additionally, ocean warming has affected a number of large marine ecosystems worldwide (Lyman
55 et al., 2010; Rhein et al., 2014). According to the IPCC Fifth Assessment Report, for example, the
56 upper 75 m of the global ocean has warmed at a rate of about 0.11°C per decade from 1971 to 2010
57 (Rhein et al., 2014). Owing to a combination of species' range shifts derived from climate change and
58 arrivals of new species, changes in marine communities are often detected in coastal regions
59 (Stachowicz et al., 2002; Perry et al., 2005; Cheung et al., 2009; Raitos et al., 2010; Sorte et al.,
60 2010). Previous studies have confirmed that native and invasive species have different responses to
61 environmental stressors; often, but not always, invasive species exhibit broader ecological tolerance,
62 thus ocean warming can result in superior performance of the latter over the former (Stachowicz et
63 al., 2002; Braby and Somero, 2006; Fields et al., 2006; Sorte et al., 2010; Anacleto et al., 2014). For
64 instance, Stachowicz et al. (2002) demonstrated that, compared with native ascidians, ocean warming
65 was expected to facilitate an earlier and more intense recruitment, as well as a higher growth rate, of

66 introduced ascidians, which might lead to changes in benthic community structure. Sorte et al. (2010)
67 also found that introduced species had higher thermal tolerance, survival, and growth than natives in a
68 marine fouling community, and accordingly they suggested that introduced species were likely to
69 dominate the fouling community with ocean warming. Considering the great susceptibility of marine
70 habitats to biological invasions jointly caused by high propagule pressure (i.e., introduction effort) as
71 a result of shipping activities and warming as a result of climate change, it is important to identify
72 potential distributions of marine invaders under present and future climate conditions for
73 implementation of management strategies at early invasion stages.

74 A large number (> 80 species globally) of ascidians (Chordata, Tunicata) are notorious invasive
75 species, affecting marine ecosystem functioning, local biodiversity, and industries such as
76 aquaculture and fisheries owing to their superior competitive ability, growth rate, and broad
77 environmental tolerance (Blum et al., 2007; Lambert, 2007; Shenkar and Swalla, 2011; Aldred and
78 Clare, 2014; Zhan et al., 2015). Ascidians generally have limited natural dispersal ability, with the
79 recent large-scale spread primarily attributed to human-mediated activities such as shipping and
80 mariculture (Lambert, 2001; Marins et al., 2010; Zhan et al., 2015). Thus far, few studies have been
81 conducted to map areas susceptible to ascidian invasions (but see Herborg et al., 2009; Locke, 2009;
82 Madariaga et al., 2014; Lins et al., 2018). Additionally, despite the recognition that climate change
83 may favour invasions by ascidians (Stachowicz et al., 2002; Sorte et al., 2010; Rius et al., 2014), its
84 effects on ascidian distributions have received relatively little attention (but see Goldsmit et al.,
85 2018). The objective of the present study is to investigate the impacts of climate changes on habitat
86 suitability of eight globally-distributed invasive ascidians: *Botrylloides violaceus*, *Botryllus*
87 *schlosseri*, *Ciona savignyi*, *Didemnum vexillum*, *Microcosmus squamiger*, *Molgula manhattensis*,
88 *Styela clava*, *Styela plicata*. We chose these invasive ascidians as they have wide ranges of
89 distribution, high availability of occurrence data, and great impacts on recipient ecosystems (Zhan et

90 al., 2015). To analyse the impact of climate changes on the potential distribution of these invaders, we
91 used ensemble species distribution models (SDMs). SDMs are a powerful tool to estimate species
92 habitat suitability by capturing the relationship between species distribution data and environmental
93 predictor variables (Guisan and Thuiller, 2005; Guisan et al., 2017). Recently, SDMs have been
94 increasingly used to examine climate change impacts on marine species, including invasive species
95 (e.g., Assis et al., 2018a; Buonomo et al., 2018; Goldsmit et al., 2018; Moraitis et al., 2018; de la Hoz
96 et al., 2019). For instance, Goldsmit et al. (2018) used SDMs to study impacts of climate changes on
97 potential distributions of eight aquatic invasive species in the Canadian Arctic, and found that climate
98 changes could result in poleward gains in habitat suitability.

99 Here, we aim to substantially expand current knowledge about the present-day and future global
100 distributions of the aforementioned invasive ascidians. Specifically, we (1) constructed ensemble
101 SDMs for each ascidian species by using species distribution data and marine predictor variables; (2)
102 evaluated relative contribution of each predictor variable to ascidian distributions to identify critical
103 variables regulating ascidian distributions; and (3) predicted habitat suitability for each ascidian
104 species under present and projected future climatic scenarios. Results of our study have important
105 implications for prioritizing resource allocation for the prevention and control of invasive ascidians
106 under a changing climate.

107

108 **2 MATERIALS AND METHODS**

109 **2.1 Study area and species occurrence records**

110 Several previous studies have highlighted that the extent of study area can influence the outcome of
111 SDMs (VanDerWal et al., 2009; Barve et al., 2011), thus it is a good practice to consider spatial
112 extent of the study area (Lins et al., 2018). Ascidians are mainly distributed in near-shore waters, thus
113 as in Lins et al. (2018), we considered only areas within the Exclusive Economic Zone (i.e., within

114 370 km of the coast).

115 Georeferenced occurrence records of each ascidian species were collected from the literature and
116 multiple online databases, including the Global Biodiversity Information Facility
117 (<http://www.gbif.org>) (GBIF.org, 2019), the Ocean Biogeographic Information System
118 (<http://iobis.org>) (OBIS, 2019), the NBN Atlas (<https://nbnatlas.org>) (NBN Atlas, 2019), the USGS
119 Biodiversity Information Serving Our Nation (<https://bison.usgs.gov>) (U.S. Geological Survey,
120 2019), the Atlas of Living Australia (<http://www.ala.org.au>) (Atlas of Living Australia, 2019), and
121 the Archive for Marine Species and Habitats Data (www.dassh.ac.uk). All above online databases
122 were accessed on November 20, 2019. Previous studies have identified the problem posed by
123 sampling bias in species occurrence records and the need to reduce it (Syfert et al., 2013; Boria et al.,
124 2014). In order to match with the spatial resolution of marine predictor variables (see section 2.2 for
125 details), we randomly selected only one occurrence record per 5 arcminute grid cell. After this data
126 cleaning procedure, a total of 3,189 occurrence records (ranging from 77 to 1,367 records per species;
127 Supporting Information Fig. S1a-S8a) were retained for downstream analyses.

128

129 **2.2 Current and future marine predictor variables**

130 Habitat suitability of marine organisms can be accurately predicted by a few variables (Belanger et
131 al., 2012; Bosch et al., 2018; Goldsmit et al., 2018). Given the information available under present
132 and future scenarios, 20 predictor variables were considered: water depth, distance to the shore, and
133 annual mean and range values (minimum values, maximum values, maximum values - minimum
134 values, average of the minimum and maximum values per year) of sea surface temperature, salinity,
135 and current velocity (see Assis et al., 2018b for details; Supporting Information Fig. S9). Water depth
136 and distance to the shore were obtained from the Global Marine Environment Datasets
137 (<http://gmed.auckland.ac.nz>) (Basher et al., 2014), while the other 18 environmental variables were

138 downloaded from Bio-ORACLE v2.0 (<http://www.bio-oracle.org>) (Assis et al., 2018b). Present
139 marine environmental predictors from Bio-ORACLE v2.0 represent average values for the period
140 2000 -2014 (Assis et al., 2018b). Collinearity of predictor variables can severely influence the
141 parameter estimates in a regression framework (Dormann et al. 2013). We therefore estimated
142 collinearity of the 20 predictor variables by calculating Pearson's correlation coefficients (r) and
143 selected only one among highly correlated variables (i.e., $|r| > 0.7$, Dormann et al. 2013);
144 consequently, nine predictor variables (i.e. water depth, distance to shore, annual mean temperature,
145 range values of temperature, annual mean salinity, range values of salinity, annual mean current
146 velocity, maximum values of current velocity, and minimum values of current velocity) were used to
147 develop SDMs (Supporting Information Fig. S9). Water depth and distance to the shore were
148 included in our analyses since SDMs without considering these two variables would fail to
149 distinguish the known distribution patterns of ascidians (Supporting Information Fig. S1c-S8c).

150 Future projections of the seven environmental predictor variables retained for 2050s (2040-2050)
151 and 2100s (2090-2100) under four greenhouse gas emission scenarios [i.e., representative
152 concentration pathway (RCP), RCP26, RCP45, RCP60, and RCP85] were also obtained from Bio-
153 ORACLE v2.0 (Assis et al., 2018b). Thus far, there is no available dataset for future water depth and
154 distance to the shore; therefore, in this study, we assume that the two geographical variables, water
155 depth and distance to the shore, will remain constant under future conditions. Although we
156 acknowledge that climate change is expect to result in sea-level rise and the two geographical
157 variables will change accordingly in the future, our SDM projections can still provide useful
158 information about ascidian invasion risks. For the purpose of reducing uncertainties, three
159 atmosphere-ocean general circulation models (i.e., CCSM4, HadGEM2-ES, MIROC5) were
160 considered and their average values were used to represent future climate conditions (Assis et al.,
161 2018b).

162

163 **2.3 Modelling procedures**

164 A variety of SDM algorithms have been developed so far, but inter-algorithmic variation is still the
165 highest source of uncertainty in future projections of species ranges (Thuiller et al., 2019). Therefore,
166 we used an ensemble modelling approach, which is acknowledged as preferable than the application
167 of a single algorithm, owing to its ability to combine results of different models, to account for the
168 prediction uncertainties (Araújo and New, 2007; Guisan et al., 2017). We considered ten modelling
169 algorithms with their default settings in the “biomod2” R package: artificial neural network (ANN),
170 classification tree analysis (CTA), flexible discriminant analysis (FDA), generalized additive model
171 (GAM), generalized boosting model (GBM), generalized linear model (GLM), multiple adaptive
172 regression splines (MARS), maximum entropy (Maxent), random forest (RF), and surface range
173 envelop (SRE) (Thuiller et al., 2014; Guisan et al., 2017). Several of these algorithms utilize species
174 presence-absence (1-0) data. True absence data is always difficult to acquire, thus we adopted 10,000
175 randomly generated pseudo-absence points within the study area as an alternative (Thuiller et al.,
176 2014; Guisan et al., 2017). A five-fold cross-validation scheme was applied to estimate predictive
177 performances of the ten SDM algorithms: each algorithm was trained using 80% of the data and
178 tested using the remaining 20% (Thuiller et al., 2014; Guisan et al., 2017). To account for slight
179 differences in the predictions caused by stochasticity in some of the algorithms, this procedure was
180 repeated ten times for each algorithm. Predictive abilities of different algorithms were evaluated by
181 two criteria: true skill statistics (TSS) (Allouche et al., 2006) and area under the receiver operating
182 characteristic curve (AUC) (Swets, 1988). The TSS values range from -1 to 1, where a value ≤ 0
183 indicates that the model gives a random prediction, and a value of 1 indicates a perfect model
184 performance (Landis and Koch, 1977). The AUC scores range from 0 to 1, with values < 0.5
185 indicating performance worse than random, a value of 0.5 indicating predictions no better than

186 random discrimination, and 1 representing perfect discrimination (Swets, 1988; Allouche et al.,
187 2006). Algorithms with TSS > 0.75 and AUC > 0.90 were further considered in this study (Landis and
188 Koch, 1977; Swets, 1988). The relative contribution of each predictor variable on ascidian
189 distribution was assessed by a randomisation approach (Thuiller et al., 2014; Guisan et al., 2017).
190 Committee averaging ensemble models were developed by using all data, which in turn were used to
191 map the habitat suitability of ascidians under present and future climate scenarios. The committee
192 averaging method represents the level of agreement among binary predictions of suitability from the
193 different single algorithms (Thuiller et al., 2014; Guisan et al., 2017). In order to establish a threshold
194 for declaring an area as suitable habitat, the continuous predictions of habitat suitability, which
195 ranged from 0 to 1, were converted into binary maps by selecting probability thresholds maximizing
196 the TSS (Jiménez-Valverde and Lobo, 2007; Thuiller et al., 2014; Guisan et al., 2017). Thus, we did
197 not adopt a fixed threshold value, but rather sought to find an optimal threshold for each species. The
198 coefficient of variation across single SDM predictions was calculated to estimate uncertainty among
199 model outputs (Thuiller et al., 2014; Guisan et al., 2017). Previous studies have demonstrated that
200 species dispersal capability can influence SDM projections (Guisan et al., 2017). In this study, we
201 estimated habitat suitability of ascidians assuming no dispersal limitations (also known as unlimited
202 dispersal ability hypothesis) – a widely used hypothesis: species have unlimited dispersal ability thus
203 can occur in climatic suitable areas. To estimate the range size of suitable habitats, projections in
204 geographic coordinate system were transformed to the Lambert Cylindrical Equal Area projection
205 with a grid cell resolution of 10 km x 10 km. All analyses were carried out in R 3.4.3 (R Core Team,
206 2017).

207

208 **3 RESULTS**

209 **3.1 Predictive accuracy of SDMs and contribution of predictor variables**

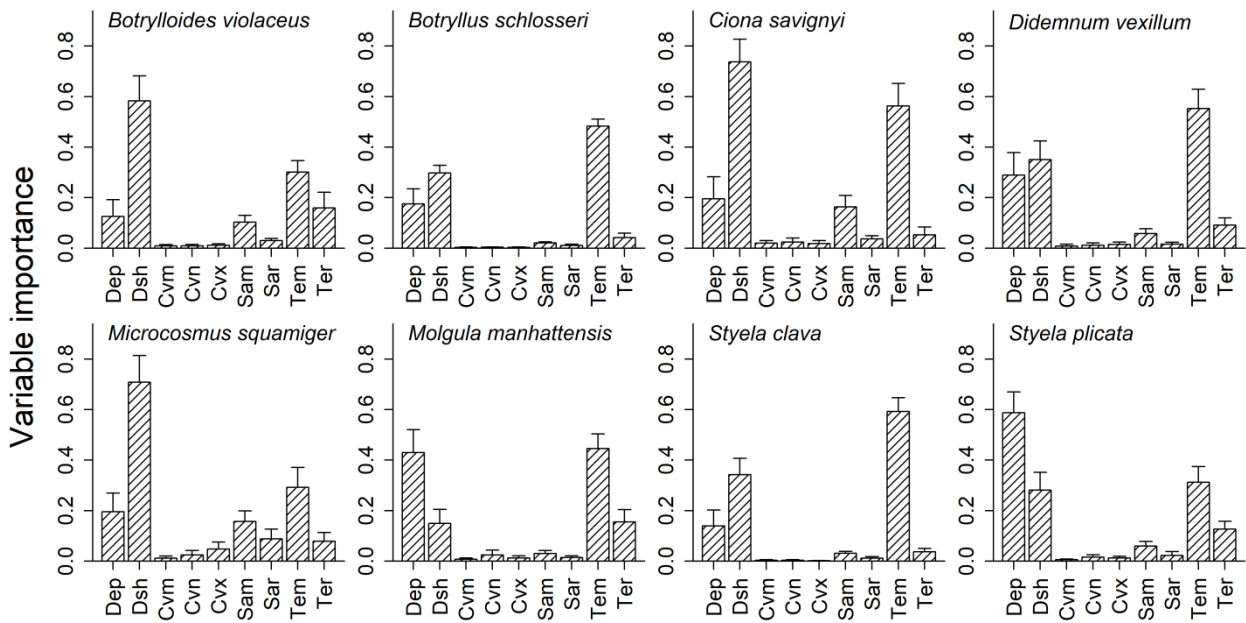
210 AUC and TSS results demonstrated that predictive abilities of SDMs varied among different
 211 modelling algorithms and that all algorithms except GAM, Maxent and SRE had excellent predictive
 212 performance for all eight ascidian species (Supporting Information Table S1, S2). Therefore, the
 213 seven best-performing algorithms, including ANN, CTA, FDA, GBM, GLM, MARS, and RF, were
 214 selected to evaluate variable importance and to construct ensemble SDMs. The ensemble SDMs
 215 exhibited excellent predictive power for all eight ascidians as evidenced by the high AUC (> 0.99)
 216 and TSS (> 0.94) values (Table 1). Results of relative contributions of the nine predictor variables to
 217 the potential distributions of ascidians suggest that despite the fact that the eight ascidian species have
 218 different environmental requirements, water depth, distance to the shore, and annual mean sea surface
 219 temperature were consistently identified as the three most important variables for all species tested
 220 (overall means of importance = 0.267, 0.431, and 0.443, respectively), followed by range of annual
 221 mean surface temperature and mean salinity (mean importance across species: 0.093 and 0.078);
 222 whereas mean current velocity, minimum current velocity, maximum current velocity, and range of
 223 annual sea surface salinity consistently contributed least to the distributions (mean importance =
 224 0.008, 0.014, 0.015, and 0.028, respectively; Fig. 1).

225
 226 **Table 1** Predictive performance of ensemble species distribution models for eight ascidian species
 227 and suitable habitat ranges of each species under present-day climate. TSS: true skill statistics; AUC:
 228 area under the receiver operating characteristic curve. The predictive abilities are expressed as mean
 229 values \pm standard error. The range of suitable habitat is represented by the number of raster cells (i.e.,
 230 100 km²) predicted to be suitable for each species.

Species	AUC	TSS	Number of raster cells
<i>Botrylloides violaceus</i>	0.992 (\pm 0.001)	0.959 (\pm 0.005)	22,644
<i>Botryllus schlosseri</i>	0.992 (\pm 0.001)	0.948 (\pm 0.001)	28,624

<i>Ciona savignyi</i>	0.999 (\pm 0.000)	0.993 (\pm 0.004)	4,048
<i>Didemnum vexillum</i>	0.996 (\pm 0.001)	0.972 (\pm 0.004)	14,747
<i>Microcosmus squamiger</i>	0.996 (\pm 0.002)	0.965 (\pm 0.014)	5,904
<i>Molgula manhattensis</i>	0.994 (\pm 0.001)	0.956 (\pm 0.003)	37,744
<i>Styela clava</i>	0.995 (\pm 0.001)	0.966 (\pm 0.001)	15,915
<i>Styela plicata</i>	0.993 (\pm 0.001)	0.960 (\pm 0.004)	28,100

231



232

233 **Fig. 1** Relative contributions of the nine predictor variables to distributions of eight ascidians. Dep:
 234 water depth, Dsh: distance to the shore, Cvm: mean current velocity, Cvn: minimum current velocity,
 235 Cvx: maximum current velocity, Sam: annual mean salinity, Sar: range of annual mean salinity, Tem:
 236 annual mean sea surface temperature, Ter: range of annual mean sea surface temperature. Data is
 237 expressed as mean values \pm standard error.

238

239 3.2 Habitat suitability under present-day climates

240 The coefficient of variation of species habitat suitability predicted by single SDMs showed that

241 variability in species occurrence probability within suitable ranges was relatively small and
242 significantly lower than that within unsuitable ranges (Supporting Information Fig. S1b-S8b). The
243 eight ascidians were predicted to have different ranges of suitable habitat under present-day climates:
244 *M. manhattensis* has the largest suitable habitat followed by *B. schlosseri*, *S. plicata*, and *B. violaceus*,
245 while suitable ranges of *C. savignyi* and *M. squamiger* were predicted to be the smallest (Table 1).
246 Interestingly, the eight ascidians showed important differences in the distribution of suitable areas.
247 For example, in Europe, the suitable habitats of *B. violaceus* and *D. vexillum* were predicted to occur
248 mainly along coastal areas of Atlantic side of the north Iberian Peninsula, Atlantic coast of France, the
249 United Kingdom, Ireland, Belgium, Netherlands Denmark, and Norway, whereas coastal areas of the
250 Mediterranean Sea were most suitable for *M. squamiger* (Supporting Information Fig. S1a-S8a).
251 Despite the different geographical ranges of climatically suitable habitats, the eight ascidians all
252 preferred shallow, nearshore waters. It is important to note that under present-day conditions, these
253 species have not yet fully occupied their predicted suitable habitats (Supporting Information Fig. S1a-
254 S8a). For instance, *B. violaceus*, *D. vexillum*, and *S. clava* have not been reported in the South
255 America, though southern coastal Argentina and Chile present suitable habitats for these species
256 (Supporting Information Fig. S1a, S4a, S7a). According to our predictions, a number of coastal
257 regions have high susceptibility to invasions by the studied ascidians, including the coastal areas of
258 China, Japan, Australia, New Zealand, North America, southern South America, the Mediterranean
259 Sea, and the Atlantic coast of Europe. In contrast, invasion risk of ascidians in Africa was much lower
260 than that in the regions mentioned above (Supporting Information Fig. S1a-S8a, S10).

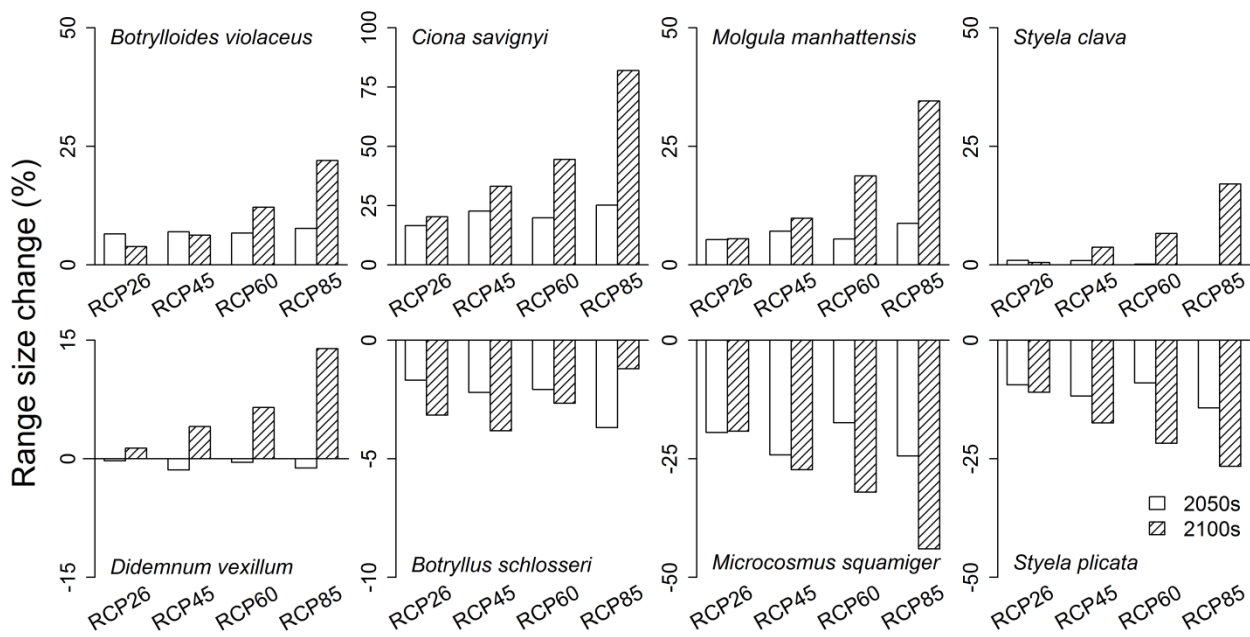
261

262 **3.3 Impacts of climate changes on ascidian distributions**

263 The eight ascidians responded differently to future climate changes (Fig. 2). The range size of *D.*
264 *vexillum* was predicted to contract in 2050s but expand in 2100s under the four RCP scenarios; the

265 range sizes were expected to decrease for *B. schlosseri*, *M. squamiger*, and *S. plicata*, but expand for
 266 the other four species under future climate conditions (Fig. 2). Regardless of the time periods and
 267 RCP scenarios selected, *C. savignyi* was predicted to experience the highest habitat expansion, from
 268 16.5% (RCP26 in 2050s) to 82.0% (RCP85 in 2100s). Our results also showed that climate changes
 269 would likely lead to greater habitat contraction in *M. squamiger* (from 17.4% decrease under RCP60
 270 in 2050s to 44.0% decrease under RCP85 in 2100s) (Fig. 2).

271



272

273 **Fig. 2** Range size changes of the eight ascidians under future climates. RCP: representative
 274 concentration pathway. 2050s: 2040-2050, 2100s: 2090-2100.

275

276 Here we used the results for the 2050s under an intermediate greenhouse gas emission scenario
 277 (i.e., RCP45) as an example to illustrate potential climate change impacts on ascidian distributions.
 278 Under these plausible conditions, an extensive part of European coasts was predicted to be suitable
 279 for the eight ascidian species (Fig. 3, Table 2). These models highlighted that the northern Atlantic
 280 coast was more susceptible to invasions, especially by *B. violaceus*, *B. schlosseri*, *D. vexillum*, *M.*

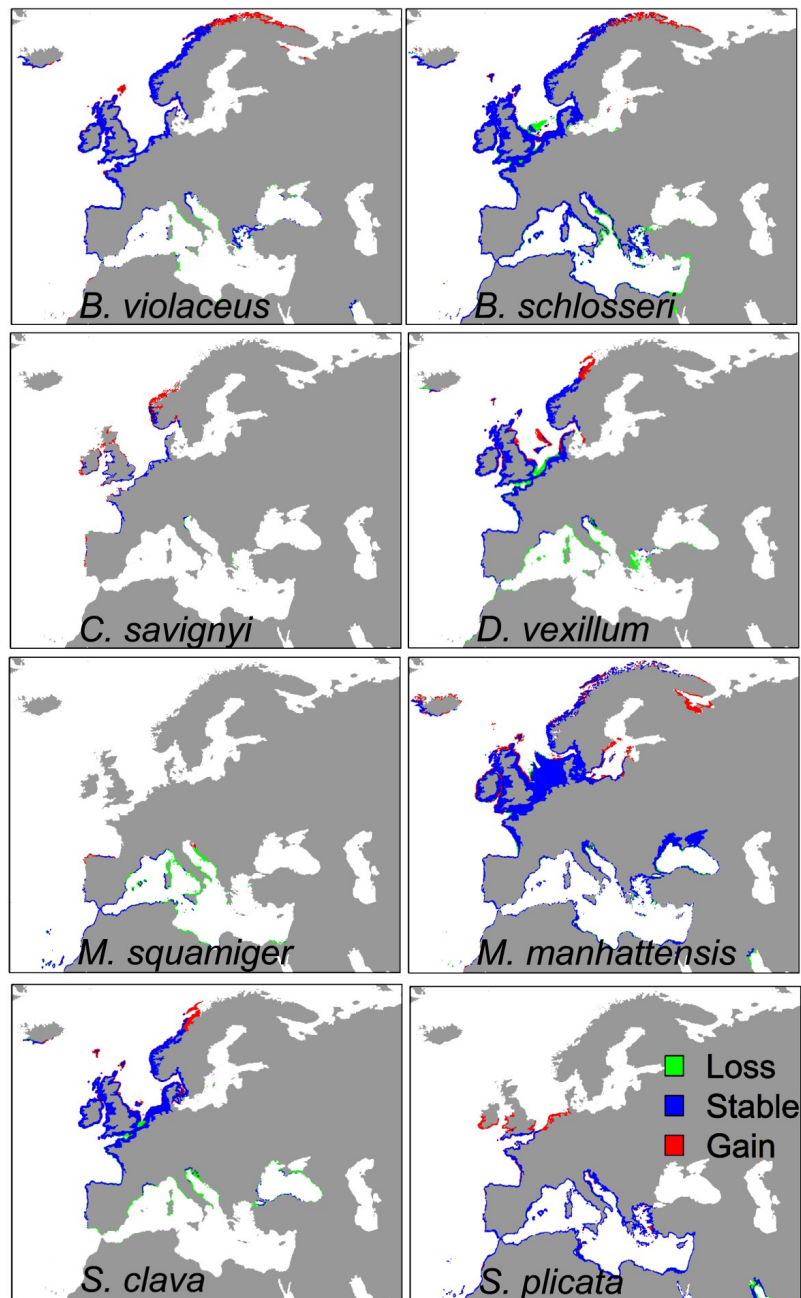
281 *manhattensis*, and *S. clava* (Fig. 3, Table 2). Additional spread of *S. plicata* was forecasted to be
 282 limited to the United Kingdom, Ireland and the Netherlands. However, species range increases in
 283 Northern Europe may be offset by losses in the southern part of the continent owing to reduced
 284 suitability (Table 2). For example, suitable habitat along the Mediterranean Sea was likely to decrease
 285 under RCP45 in 2050s for all ascidians except *C. savignyi* and *S. plicata*, whose habitats were
 286 expected to remain nearly unchanged (Fig. 3).

287

288 **Table 2** Suitable habitat ranges of each species under present-day climate and range size change
 289 (percentage values in parentheses) under RCP45 in 2050s. Four regions (i.e. Americas, Europe,
 290 Western Pacific, and Africa) were divided as shown in Figure 3, 4, 5, and S10. Range size change was
 291 calculated as: (suitable range under RCP45 in 2050s – present-day suitable range)/present-day
 292 suitable range. Suitable habitat range is represented by the number of raster cells (i.e., 100 km²)
 293 predicted to be suitable for each species.

Species	Present-day suitable range and range change under RCP45 in 2050s			
	Americas	Europe	Western Pacific	Africa
<i>B. violaceus</i>	8,966 (9.6%)	5,441 (7.2%)	7,349 (5.6%)	694 (-12.2%)
<i>B. schlosseri</i>	8,591 (12.3%)	11,767 (-9.5%)	7,170 (-6.0%)	774 (-12.5%)
<i>C. savignyi</i>	1,725 (45.4%)	825 (55.3%)	1,504 (-16.6%)	24 (-33.3%)
<i>D. vexillum</i>	5,327 (18.1%)	5,484 (-6.6%)	3,471 (-22.4%)	372 (-22.8%)
<i>M. squamiger</i>	1,333 (-20.4%)	1,780 (-49.7%)	1,806 (-1.9%)	769 (-27.4%)
<i>M. manhattensis</i>	14,378 (12.3%)	12,237 (6.0%)	10,402 (1.6%)	630 (-20.5%)
<i>S. clava</i>	5,111 (26.9%)	5,774 (-3.6%)	4,543 (-20.1%)	355 (-26.5%)
<i>S. plicata</i>	9,135 (-17.3%)	5,557 (9.8%)	9,679 (-9.2%)	2,961 (-32.3%)

294

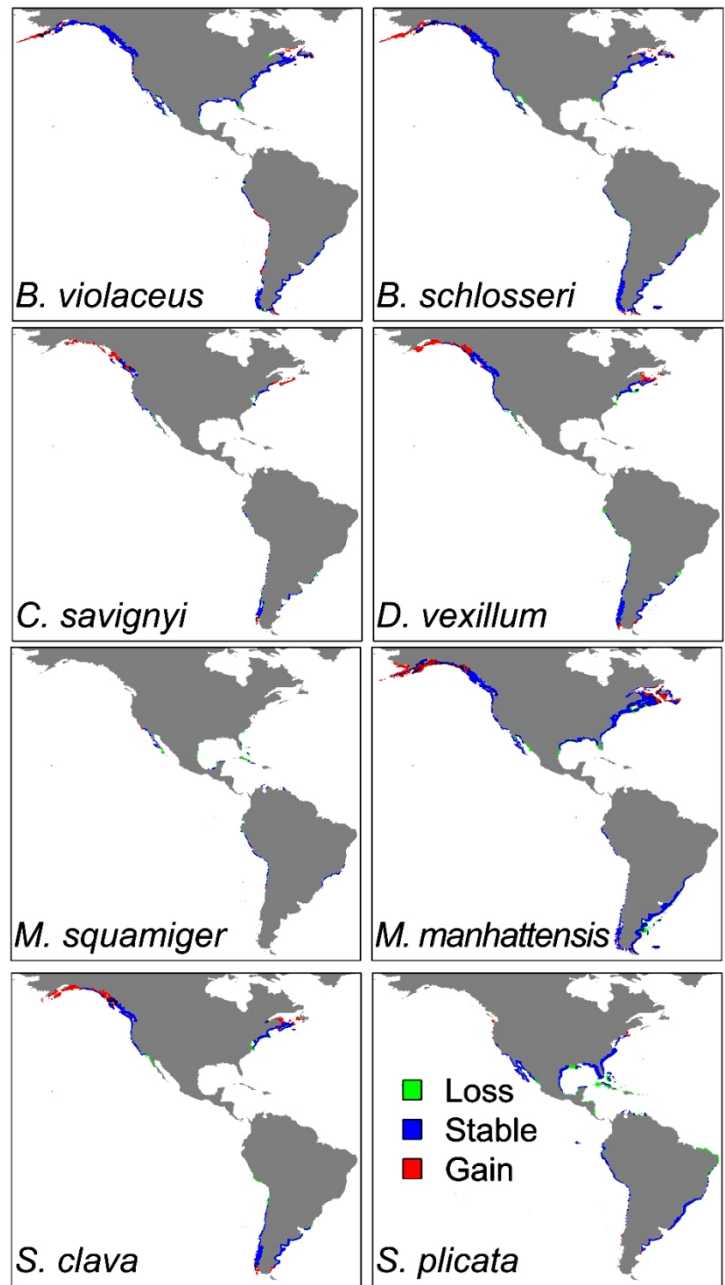


295

296 **Fig. 3** Predicted range shifts of the eight ascidians in Europe in 2050s under RCP45 scenario. RCP:
 297 representative concentration pathway. 2050s: 2040-2050. Stable areas (in blue) indicate habitats that
 298 are predicted to be suitable under both present-day and future climates; loss areas (in green) show
 299 areas which are predicted to be no longer suitable in the future; gain areas (in red) represent habitats
 300 that are predicted to become suitable in the future.

301

302 Concerning the coasts of North and South America, model predictions highlighted that large
303 coastal regions – except for the tropics – would be suitable for all ascidians (Fig. 4, Table 2). Suitable
304 habitats of *M. squamiger* and *S. plicata* were predicted to contract under future climates (Table 2).
305 Habitats of six species, including *B. violaceus*, *B. schlosseri*, *C. savignyi*, *D. vexillum*, *M.*
306 *manhattensis*, and *S. clava*, were expected to exhibit a poleward expansion, especially along the Gulf
307 of Alaska, Gulf of Saint Lawrence, and Patagonia (Fig. 4). Most ascidians were projected to
308 encounter suitable habitat only north of the Tropic of Cancer in the northern hemisphere and south of
309 the Tropic of Capricorn in the southern hemisphere; north of the Tropic of Capricorn, all species
310 except *S. plicata* were expected to experience suitable habitats only on the west coast, if at all (Fig. 4).



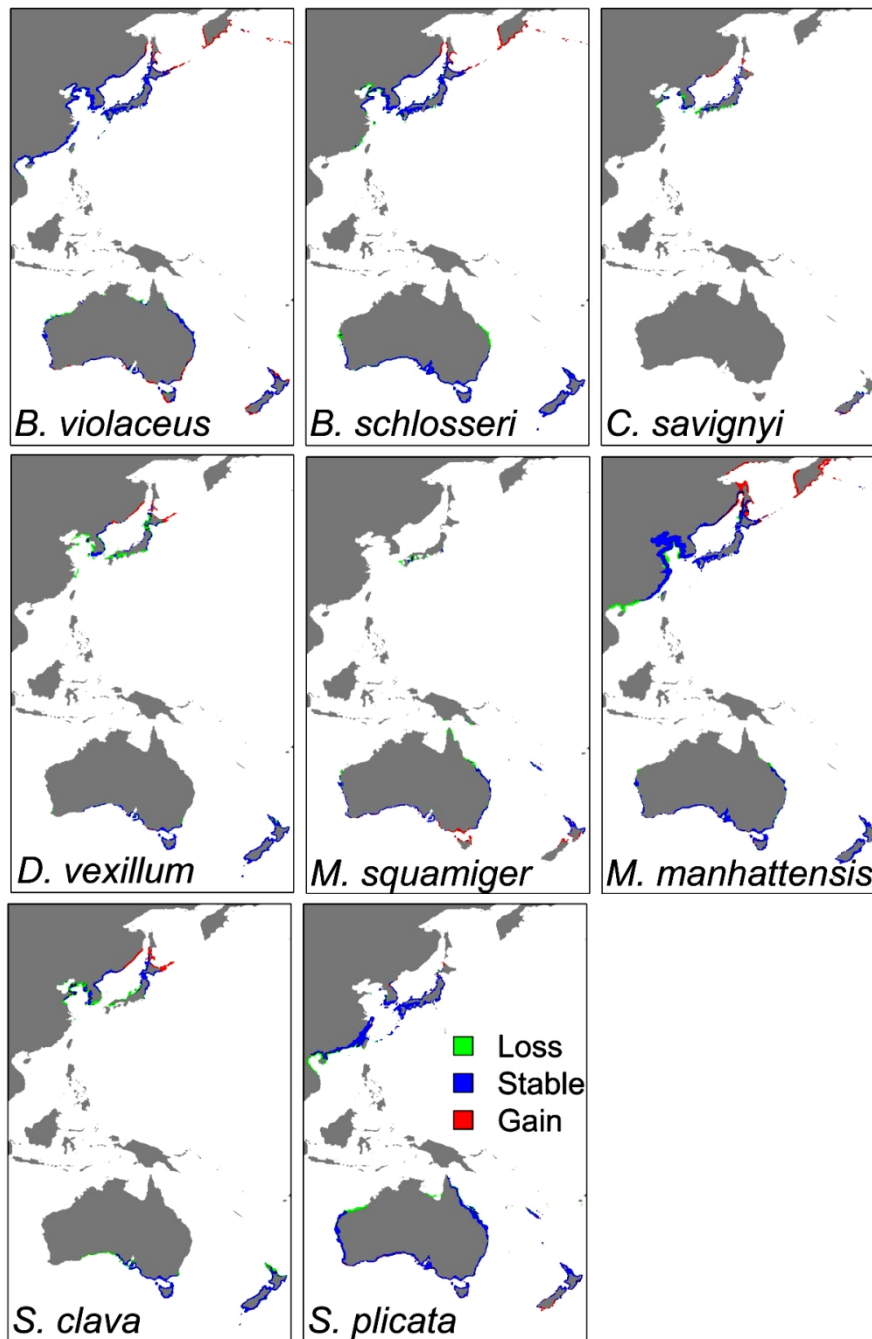
311

312 **Fig. 4** Predicted range shifts of the eight ascidians in the Americas in 2050s under RCP45 scenario.

313 RCP: representative concentration pathway. 2050s: 2040-2050. Stable areas (in blue) indicate
 314 habitats that are predicted to be suitable under both present-day and future climates; loss areas (in
 315 green) show areas which are predicted to be no longer suitable in the future; gain areas (in red)
 316 represent habitats that are predicted to be suitable in the future.

317

318 The coasts of China, Korea, and Japan were predicted under future climate change scenarios to
319 be suitable habitats for all eight ascidians. Seven species, including *B. violaceus*, *B. schlosseri*, *C.*
320 *savignyi*, *D. vexillum*, *M. manhattensis*, *S. clava*, and *S. plicata*, will generally lose habitat suitability
321 in East Asia and, owing to climate changes, all these species except *S. plicata* would extend their
322 habitats further north in Hokkaido in Northern Japan (Fig. 5). The coasts of Australia and New
323 Zealand were expected to remain susceptible to invasions by all ascidians in 2050s, with little
324 expected changes in patterns (Fig. 5). *M. squamiger* and *S. plicata* habitat might expand to include
325 Tasmania and adjacent coastal mainland Australia, as well as the South Island of New Zealand. In
326 addition, *S. plicata* would experience loss of suitable habitats in some regions of Northern Australia.



327

328 **Fig. 5** Predicted range shifts of the eight ascidians along coastal areas of the Western Pacific in 2050s
 329 under RCP45 scenario. RCP: representative concentration pathway. 2050s: 2040-2050. Stable areas
 330 (in blue) indicate habitats that are predicted to be suitable under both present-day and future climates;
 331 loss areas (in green) show areas which are predicted to be no longer suitable in the future; gain areas
 332 (in red) represent habitats that are predicted to be suitable in the future.

333

334 **4 Discussion**

335 In this study, we developed ensemble SDMs for eight invasive ascidian species and investigated
336 climate change impacts on their global potential distributions. Ensemble SDMs showed good
337 predictive abilities and indicated that the eight ascidians have not yet colonized the full extent of their
338 present-day suitable habitats worldwide. Our models also predicted that these species would behave
339 differently under future climate scenarios. Our results hold important implications for developing
340 management strategies for these highly invasive ascidians.

341 Among the nine predictor variables chosen to construct SDMs, distance to the shore, water depth,
342 and annual mean sea surface temperature were the top three influential predictors of ascidian
343 distributions. As these species are mainly restricted to shallow, nearshore habitats, it was not
344 surprising that two geographical variables were predicted to play critical roles in regulating their
345 distributions. Our finding regarding the importance of annual mean sea surface temperature is in
346 agreement with previous studies (Belanger et al., 2012; Bosch et al., 2018; Goldsmit et al., 2018).
347 Furthermore, Belanger et al. (2012) demonstrated that mean annual temperature was the most
348 important predictor variable regulating benthic marine biogeographic structure. Similarly, using
349 SDMs, Bosch et al. (2018) provided convincing evidence that the mean sea surface temperature was
350 the most relevant predictor of global distributions for 514 marine species.

351 Water salinity also strongly influences ascidian development and distributions (Thiyagarajan and
352 Qian, 2003; Epelbaum et al., 2009; Locke and Carman, 2009; Nagar and Shenkar, 2016). In our study,
353 ensemble SDMs highlighted that the effect of salinity was not nearly as strong as that of temperature
354 in any of the eight ascidian species. Such difference was mainly due to the limited variation of salinity
355 in our study areas. We focused only on coastal areas within the Exclusive Economic Zone. Within
356 this area, mean sea surface temperature was evenly distributed and covered a wide range from -1.7 to
357 30.2 °C, whereas mean sea surface salinity mainly varied only between 30 and 38‰ (Supporting

358 Information Fig. S11). This relatively minor variation in mean sea surface salinity might partly
359 account for our model's failure to highlight the importance of salinity in affecting ascidian
360 distributions.

361 According to our SDM predictions, the eight ascidians displayed different distribution patterns
362 under present-day climates (Supporting Information Fig. S1a-S8a) and were expected to respond
363 differently to future climate changes (Fig. 3-5). Under present-day climates, predicted suitable
364 habitats of the eight ascidians were often larger than their current known distribution ranges. This
365 finding is consistent with several previous SDM studies on ascidians (Herborg et al., 2009; Goldsmit
366 et al., 2018; Lins et al., 2018). Several possible factors including dispersal limitation and sampling
367 bias have been proposed to explain this phenomenon (see Goldsmit et al. 2018). Owing to intensive
368 human activities such as global shipping, invasion risks of *M. manhattensis*, *B. schlosseri*, *B.*
369 *violaceus*, *S. plicata*, *D. vexillum*, and *S. clava* induced by such activities were expected to be high
370 due to their large area of suitable habitats, while risks of *M. squamiger* and *C. savignyi* spread were
371 relatively low (Fig. 3-5). These findings are troubling because several biological features of ascidians
372 such as a relative short planktonic larval phase (usually minutes to several days) lead to a high level of
373 dispersal limitation, particularly at regional and continental scales (Zhan et al., 2015). Thus, great
374 care must be taken to ensure that intensive human activities such as shipping and aquaculture do not
375 facilitate further spread of these invasive species to uncolonized areas.

376 Future climate changes are likely to result in changes in habitat suitability. Overall, we predicted
377 a poleward expansion of these warm-temperate species, with loss of suitable habitats on the warmer
378 trailing edges. This is a feature commonly predicted for marine organisms (Perry et al., 2005; Cheung
379 et al., 2009) and for ascidians as well (Tracy et al., 2017). Our results support the findings by
380 Goldsmit et al. (2018), who estimated climate change impacts on habitat suitability of eight invaders
381 including *B. violaceus* in the Canadian Arctic. Their results predicted suitable habitat of *B. violaceus*

382 to increase by 17.1% under RCP45 emission scenario by mid-century, with a poleward shift. Shifts in
383 species ranges related to climate changes have been documented or projected for many marine
384 species (Perry et al., 2005; Vermeijj and Roopnarine, 2008; Cheung et al., 2009; Assis et al., 2018a;
385 Chan et al., 2019). Such distribution shifts can pose great threats to marine ecosystems by altering
386 species interactions, and to humans dependent on living marine resources. For instance, a coastal fish
387 species distributed along the west coast of southern Africa experienced a southward distributional
388 shift during ocean warming, resulting in hybridization with its local congeners (Potts et al., 2014).
389 Moreover, a ten-year study in eastern Australia demonstrated that ocean warming increased the
390 proportion of herbivorous fishes in kelp forests, which in turn led to the loss of kelp (Vergés et al.,
391 2016). Species loss as a result of direct and indirect effects of the new invaders, as well as
392 hybridization with native species on the newly colonized areas, allow biological changes to persist
393 even if the initiating driver (climate change) has waned. Further studies are required to investigate the
394 impacts of distribution shifts of invasive ascidians on native ecosystems.

395 According to our SDM predictions under future climate scenarios, four ascidians were expected
396 to expand their geographic ranges while geographical distributions of three species were likely to
397 contract. These different responses to climate changes might reflect different environmental tolerance
398 among these ascidians. It is noteworthy that the eight species investigated have a warm-temperate
399 distribution range, yet diverse responses to climate change were predicted. This may indicate the high
400 sensitivity of our modelling approach to nuances in tolerance limits of the species that can be detected
401 only after careful analysis of their distribution patterns. Similar results were also detected in other
402 aquatic organisms. For example, Van Zuiden et al. (2016) used SDMs to identify species-specific
403 responses to climate change by fishes from three thermal guilds in Ontario, Canada. Species-specific
404 environmental tolerance to temperature and salinity has been previously investigated in several
405 ascidian species (see Pineda et al., 2012; Madariaga et al., 2014; Rius et al., 2014). Further studies are

406 required to examine environmental preferences of ascidians and confirm whether these ascidians
407 display different thresholds of environmental tolerance.

408 A crucial point in all modelling approaches is the correctness of taxonomic assignments. For
409 broadly distributed taxa, there is always the possibility that unrecognized cryptic speciation can
410 confound analyses, and this is particularly true for ascidians (e.g., Teske et al., 2011; Zhan et al.,
411 2012; Pérez-Portela et al., 2013). In our target species, genetic evidence provided confidence that we
412 dealt with single species entities in most cases (*Botrylloides violaceus*, Bock et al., 2011; *Ciona*
413 *savignyi*, Griggio et al., 2014, Nydam and Harrison, 2007; *Didemnum vexillum*, Stefaniak et al., 2009;
414 *Microcosmus squamiger*, Rius et al., 2012; *Molgula manhattensis*, Haydar et al., 2011; *Styela clava*,
415 Goldstien et al., 2011; *Styela plicata*: Pineda et al., 2011). For *Botryllus schlosseri*, however, concern
416 exists about its taxonomic status and the accuracy of existing reports, as the species has been shown
417 to comprise several genetic clades (Bock et al., 2012; Nydam et al., 2017) and speciation processes
418 may be ongoing in some clades (Griggio et al., 2014). Even though reference databases may
419 confound different clades of this species complex, we are confident that most records correspond to
420 the widespread and invasive clade (i.e., Clade A in Bock et al., 2012). Thus, our results should be still
421 valid in this regard, though caution should be applied in this case. In addition, it is important to note
422 that SDMs only capture correlations between species distribution data and environmental variables
423 but do not account for different life-history characteristics (Guisan and Thuiller, 2005; Guisan et al.,
424 2017; Briscoe et al., 2019). For instance, ascidians have diverse reproductive modes (from asexual to
425 sexual reproduction) (Zhan et al., 2015) and SDMs cannot incorporate these differences. Process-
426 explicit models may represent an alternative to overcome these barriers (Briscoe et al., 2019).

427 Another important conclusion of our analyses is the contrasting distribution forecasts for South
428 America and Africa. The former presents a large fraction of already suitable habitats that have not
429 been colonized by the species studied, and was forecasted to experience poleward gains of suitable

430 habitats in the future, particularly in the Atlantic and Pacific coasts of the Patagonian region. This
431 region emerges, therefore, as a high-risk area and one suitable for enhanced surveillance and pathway
432 control. On the contrary, African coasts (excluding the Mediterranean side) have a low present-day
433 risk of invasions by the studied species and the situation is unlikely to change appreciably in the
434 future, so this continent is, for the time being, of least concern in this respect. However, important
435 shipping ports, such as those in South Africa, can change this picture rapidly as warming increases
436 (Rius et al., 2014). Consequently, those hot spots should be closely monitored.

437 Our results highlight the importance of climate change impacts on invasive ascidian distributions
438 and can be used as a guide to develop management strategies given that these organisms are among
439 the most troublesome invaders in the sea. SDM predictions indicated that invasion risks of the eight
440 ascidians were mainly concentrated along coastal areas of the Americas, Europe, East Asia, and
441 Australasia. In areas where ascidians have already become established, physical and chemical
442 eradication methods are required to protect marine ecosystems (Zhan et al., 2015). In areas less likely
443 to be suitable for ascidian colonization under future climates - such as coasts of the Mediterranean
444 Sea for *B. schlosseri* and *M. squamiger* and East Asia for *D. vexillum* and *M. manhattensis* -
445 prevention measures may be most effective. Eradication of established invasive species is very
446 difficult and always requires long-term economic and social supports, and this is also the case for
447 ascidians (e.g., Forrest and Hopkins, 2013; Sambrook et al., 2014). Therefore, effective prevention
448 approaches should focus on curtailing initial spread to uncolonized regions (Olenin et al., 2011; Zhan
449 et al., 2015). It should be noted that invasive ascidians tend to colonize artificial habitats; however,
450 we could not incorporate artificial habitats into SDMs owing to the lack of data availability.
451 Urbanized coasts may have higher risks to receive invasions in predicted suitable habitats by SDMs
452 (Airoldi et al., 2015). Consequently coasts in urbanized areas should be prioritized to conduct
453 surveillance and implement prevention programs. Environmental DNA (eDNA) has proven useful

454 for early detection of invasive species (Dejean et al., 2012; Larson et al., 2017), and Zhan et al. (2015)
455 proposed the method be used for invasive ascidians. However, additional work is required to develop
456 highly sensitive, species-specific eDNA markers for the suite of ascidians now spreading globally
457 (Simpson et al., 2017). Further global progress on limiting dispersal opportunities by ballast water
458 and hull fouling is needed to curtail spread of ascidian species.

459

460 **5 Conclusions**

461 Modelling approaches hold a great potential to optimize prevention and management decisions. In
462 this study, we found that the scope for expansion of invasive ascidian species was different and could
463 be assessed by using the ensemble SDM approach. Our study predicted where ascidian species would
464 and would not survive if introduced, and also identified high risk areas where monitoring and control
465 efforts should be concentrated. We encourage the application of modelling procedures to forecast
466 marine invasion dynamics and accordingly to develop management strategies such as early detection
467 in high risk areas.

468

469 **Acknowledgements**

470 We would like to thank all members in Zhan Laboratory for their assistance in literature review for
471 data collection. This work was supported by the National Natural Science Foundation of China (Nos.
472 31622011, 31772449) to AZ, the project CTM2017-88080 (MCIU/AEI/FEDER/UE) of the Spanish
473 Government to XT, an NSERC Discovery grant and Canada Research Chair in Aquatic Invasive
474 Species to HJM. CC was funded by National Funds through FCT, I.P., under the programme of
475 ‘Stimulus of Scientific Employment – Individual Support’ within the contract
476 ‘CEECIND/02037/2017’. DNK received funding from the ERA-Net BiodivERsA - Belmont Forum,
477 with the national funder Swiss National Foundation (20BD21_184131), part of the 2018 Joint call

478 BiodivERsA-Belmont Forum call (project ‘FutureWeb’).

479

480 **Conflict of Interest:** The authors declare that they have no conflict of interest.

481

482 **References**

483 Airoidi, L., Turon, X., Perkol-Finkel, S., & Rius, M. (2015). Corridors for aliens but not for natives:
484 effects of marine urban sprawl at a regional scale. *Diversity and Distributions*, 21, 755–768.

485 <https://doi.org/10.1111/ddi.12301>

486 Aldred, N., & Clare, A. S. (2014). Impact and dynamics of surface fouling by solitary and compound
487 ascidians. *Biofouling*, 30:259–270. <https://doi.org/10.1080/08927014.2013.866653>

488 Allouche, O., Tsoar, A., & Kadmon, R. (2006). Assessing the accuracy of species distribution
489 models: prevalence, kappa and the true skill statistic (TSS). *Journal of Applied Ecology*, 43,
490 1223–1232. <https://doi.org/10.1111/j.1365-2664.2006.01214.x>

491 Anacleto, P., Maulvault, A. L., Lopes, V. M., Repolho, T., Diniz, M., Nunes, M. L., Marques, A., &
492 Rosa, R. (2014). Ecophysiology of native and alien-invasive clams in an ocean warming context.
493 *Comparative Biochemistry and Physiology Part A: Molecular & Integrative Physiology*, 175,
494 28–37. <https://doi.org/10.1016/j.cbpa.2014.05.003>

495 Araújo, M. B., & New, M. (2007). Ensemble forecasting of species distributions. *Trends in Ecology
496 and Evolution*, 22, 42–47. <https://doi.org/10.1016/j.tree.2006.09.010>

497 Assis, J., Araújo, M. B., & Serrão, E. A. (2018a). Projected climate changes threaten ancient refugia
498 of kelp forests in the North Atlantic. *Global Change Biology*, 24, e55–e66.

499 <https://doi.org/10.1111/gcb.13818>

500 Assis, J., Tyberghein, L., Bosch, S., Verbruggen, H., Serrão, E. A., & De Clerck, O. (2018b). Bio-
501 ORACLE v2.0: Extending marine data layers for bioclimatic modelling. *Global Ecology and
502 Biogeography*, 27, 277–284. <https://doi.org/10.1111/geb.12693>

503 Atlas of Living Australia. (2019). Atlas of Living Australia website at <http://www.ala.org.au>.
504 Accessed 20 November 2019

505 Barve, N., Barve, V., Jiménez-Valverde, A., Lira-Noriega, A., Maher, S. P., Peterson, A. T.,
506 Soberón, J., & Villalobos, F. (2011). The crucial role of the accessible area in ecological niche
507 modeling and species distribution modeling. *Ecological Modelling*, 222, 1810–1819.
508 <https://doi.org/10.1016/j.ecolmodel.2011.02.011>

509 Basher, Z., Bowden, D. A., & Costello, M. J. (2014). Global marine environment dataset (GMED).
510 Version 1.0 (Rev.01.2014). Available from <http://gmed.auckland.ac.nz>.

511 Belanger, C. L., Jablonski, D., Roy, K., Berke, S. K., Krug, A. Z., Valentine, J. W. 2012. Global
512 environmental predictors of benthic marine biogeographic structure. *Proceedings of the National*
513 *Academy of Sciences*, 109, 14046–14051. <https://doi.org/10.1073/pnas.1212381109>

514 Blum, J. C., Chang, A. L., Liljeström, M., Schenk, M. E., Steinberg, M. K., & Ruiz, G. M. (2007).
515 The non-native solitary ascidian *Ciona intestinalis* (L.) depresses species richness. *Journal of*
516 *Experimental Marine Biology and Ecology*, 342, 5–14.
517 <https://doi.org/10.1016/j.jembe.2006.10.010>

518 Bock, D. G., MacIsaac, H. J., & Cristescu, M. E. (2012). Multilocus genetic analyses differentiate
519 between widespread and spatially restricted cryptic species in a model ascidian. *Proceedings of*
520 *the Royal Society B: Biological Sciences*, 279, 2377–2385.
521 <https://doi.org/10.1098/rspb.2011.2610>

522 Bock, D. G., Zhan, A., Lejeusne, C., MacIsaac, H. J., & Cristescu, M. E. (2011). Looking at both
523 sides of the invasion: patterns of colonization in the violet tunicate *Botrylloides violaceus*.
524 *Molecular Ecology*, 20, 503–516. <https://doi.org/10.1111/j.1365-294X.2010.04971.x>

525 Boria, R. A., Olson, L. E., Goodman, S. M., & Anderson, R. P. (2014). Spatial filtering to reduce
526 sampling bias can improve the performance of ecological niche models. *Ecological Modelling*,

527 275, 73–77. <https://doi.org/10.1016/j.ecolmodel.2013.12.012>

528 Bosch, S., Tyberghein, L., Deneudt, K., Hernandez, F., & De Clerck, O. 2018. In search of relevant
529 predictors for marine species distribution modelling using the MarineSPEED benchmark dataset.
530 *Diversity and Distributions*, 24, 144–157. <https://doi.org/10.1111/ddi.12668>

531 Braby, C. E., & Somero, G. N. (2006). Following the heart: temperature and salinity effects on heart
532 rate in native and invasive species of blue mussels (genus *Mytilus*). *Journal of Experimental*
533 *Biology*, 209, 2554–2566. <https://doi.org/10.1242/jeb.02259>

534 Briscoe, N. J., Elith, J., Salguero-Gomez, R., Lahoz-Monfort, J. J., Camac, J. S., Giljohann, K. M.,
535 Holden, M. H., Hradsky, B. A., Kearney, M. R., McMahon, S. M., Phillips, B. L., Regan, T. J.,
536 Rhodes, J. R., Vesk, P. A., Wintle, B. A., Yen, J. D. L., Guillera-Aroita, G. (2019). Forecasting
537 species range dynamics with process-explicit models: matching methods to applications.
538 *Ecology Letters*, 22, 1940–1956. <https://doi.org/10.1111/ele.13348>

539 Buonomo, R., Chefaoui, R. M., Lacida, R. B., Engelen, A. H., Serrão, E. A., & Airoidi, L. (2018).
540 Predicted extinction of unique genetic diversity in marine forests of *Cystoseira* spp. *Marine*
541 *Environmental Research*, 138, 119–128. <https://doi.org/10.1016/j.marenvres.2018.04.013>

542 Chan, F.T., Stanislawczyk, K., Sneekes, A.C., Dvoretzky, A., Gollasch, S., Minchin, D., David, M.,
543 Jelmert, A., Albretsen, J. & Bailey, S.A. (2019) Climate change opens new frontiers for marine
544 species in the Arctic: Current trends and future invasion risks. *Global Change Biology*, 25, 25–
545 38. <https://doi.org/10.1111/gcb.14469>

546 Cheung, W. W., Lam, V. W., Sarmiento, J. L., Kearney, K., Watson, R., & Pauly, D. (2009).
547 Projecting global marine biodiversity impacts under climate change scenarios. *Fish and*
548 *Fisheries*, 10, 235–251. <https://doi.org/10.1111/j.1467-2979.2008.00315.x>

549 de la Hoz, C. F., Ramos, E., Puente, A., & Juanes, J. A. (2019). Climate change induced range shifts
550 in seaweeds distributions in Europe. *Marine Environmental Research*. 148, 1–11.

551 <https://doi.org/10.1016/j.marenvres.2019.04.012>

552 Dejean, T., Valentini, A., Miquel, C., Taberlet, P., Bellemain, E., & Miaud, C. (2012). Improved
553 detection of an alien invasive species through environmental DNA barcoding: the example of the
554 American bullfrog *Lithobates catesbeianus*. *Journal of Applied Ecology*, 49, 953–959.
555 <https://doi.org/10.1111/j.1365-2664.2012.02171.x>

556 Dormann, C. F., Elith, J., Bacher, S., Buchmann, C., Carl, G., Carré, G., Marquéz, J. R. G., Gruber,
557 B., Lafourcade, B., Leitão, P. J., Münkemüller, T., McClean, C., Osborne, P. E., Reineking, B.,
558 Schröder, B., Skidmore, A. K., Zurell, D., & Lautenbach, S. (2013). Collinearity: a review of
559 methods to deal with it and a simulation study evaluating their performance. *Ecography*, 36, 27–
560 46. <https://doi.org/10.1111/j.1600-0587.2012.07348.x>

561 Ehrenfeld, J. G. (2010). Ecosystem consequences of biological invasions. *Annual Review of Ecology,*
562 *Evolution, and Systematics*, 41, 59–80. <https://doi.org/10.1146/annurev-ecolsys-102209-144650>

563 Epelbaum, A., Herborg, L. M., Therriault, T. W., & Pearce, C. M. (2009). Temperature and salinity
564 effects on growth, survival, reproduction, and potential distribution of two non-indigenous
565 botryllid ascidians in British Columbia. *Journal of Experimental Marine Biology and Ecology*,
566 369, 43–52. <https://doi.org/10.1016/j.jembe.2008.10.028>

567 Fields, P. A., Rudomin, E. L., & Somero, G. N. (2006). Temperature sensitivities of cytosolic malate
568 dehydrogenases from native and invasive species of marine mussels (genus *Mytilus*): sequence-
569 function linkages and correlations with biogeographic distribution. *Journal of Experimental*
570 *Biology*, 209, 656–667. <https://doi.org/10.1242/jeb.02036>

571 Forrest, B. M., & Hopkins, G. A. (2013). Population control to mitigate the spread of marine pests:
572 insights from management of the Asian kelp *Undaria pinnatifida* and colonial ascidian
573 *Didemnum vexillum*. *Management of Biological Invasions*, 4, 317–326.
574 <https://doi.org/10.3391/mbi.2013.4.4.06>

575 GBIF.org. (2019). GBIF occurrence download www.gbif.org. Accessed from R via dismo
576 (<https://CRAN.R-project.org/package=dismo>) on 2019-11-20

577 Goldsmit, J., Archambault, P., Chust, G., Villarino, E., Liu, G., Lukovich, J. V., Barber, D. G., &
578 Howland, K. L. (2018). Projecting present and future habitat suitability of ship-mediated aquatic
579 invasive species in the Canadian Arctic. *Biological Invasions*, 20, 501–517.
580 <https://doi.org/10.1007/s10530-017-1553-7>

581 Goldstien, S. J., Dupont, L., Viard, F., Hallas, P. J., Nishikawa, T., Schiel, D. R., ... & Bishop, J. D.
582 (2011). Global phylogeography of the widely introduced North West Pacific ascidian *Styela*
583 *clava*. *PLoS ONE*, 6, e16755. <https://doi.org/10.1371/journal.pone.0016755>

584 Griggio, F., Voskoboynik, A., Iannelli, F., Justy, F., Tilak, M. K., Xavier, T., ... & Gissi, C. (2014).
585 Ascidian mitogenomics: comparison of evolutionary rates in closely related taxa provides
586 evidence of ongoing speciation events. *Genome Biology and Evolution*, 6, 591–605.
587 <https://doi.org/10.1093/gbe/evu041>

588 Guisan, A., & Thuiller, W. (2005). Predicting species distribution: offering more than simple habitat
589 models. *Ecology Letters*, 8, 993–1009. <https://doi.org/10.1111/j.1461-0248.2005.00792.x>

590 Guisan, A., Thuiller, W., & Zimmermann, N. E. (2017). *Habitat Suitability and Distribution Models:*
591 *With Applications in R*. Cambridge University Press, Cambridge.

592 Haydar, D., Hoarau, G., Olsen, J. L., Stam, W. T., & Wolff, W. J. (2011). Introduced or glacial relict?
593 Phylogeography of the cryptogenic tunicate *Molgula manhattensis* (Ascidiacea, Pleurogona).
594 *Diversity and Distributions*, 17, 68–80. <https://doi.org/10.1111/j.1472-4642.2010.00718.x>

595 Herborg, L. M., O'Hara, P., & Therriault, T. W. (2009). Forecasting the potential distribution of the
596 invasive tunicate *Didemnum vexillum*. *Journal of Applied Ecology*, 46, 64–72.
597 <https://doi.org/10.1111/j.1365-2664.2008.01568.x>

598 Jiménez-Valverde, A., & Lobo, J. M. (2007). Threshold criteria for conversion of probability of

599 species presence to either–or presence–absence. *Acta Oecologica*, 31(3), 361–369.
600 <https://doi.org/10.1016/j.actao.2007.02.001>

601 Kaluza, P., Kölzsch, A., Gastner, M. T., & Blasius, B. (2010). The complex network of global cargo
602 ship movements. *Journal of the Royal Society Interface*, 7, 1093–1103.
603 <https://doi.org/10.1098/rsif.2009.0495>

604 Kozubíková, E., Filipová, L., Kozák, P., Ďuriš, Z., Martín, M. P., Diéguez-Uribeondo, J., Oidtmann,
605 B., & Petrušek, A. (2009). Prevalence of the crayfish plague pathogen *Aphanomyces astaci* in
606 invasive American crayfishes in the Czech Republic. *Conservation Biology*, 23, 1204–1213.
607 <https://doi.org/10.1111/j.1523-1739.2009.01240.x>

608 Lambert, G. (2001). A global overview of ascidian introductions and their possible impact on the
609 endemic fauna. In: Sawada, H., Yokosawa, H., & Lambert, C. C. (eds), *The Biology of*
610 *Ascidians*. Tokyo, Springer-Verlag, 249–257.

611 Lambert, G. (2007). Invasive sea squirts: a growing global problem. *Journal of Experimental Marine*
612 *Biology and Ecology*, 342, 3–4. <https://doi.org/10.1016/j.jembe.2006.10.009>

613 Landis, J. R., & Koch, G. G. (1977). The measurement of observer agreement for categorical data.
614 *Biometrics*, 33, 159–174. <https://doi.org/10.2307/2529310>

615 Larson, E. R., Renshaw, M. A., Gantz, C. A., Umek, J., Chandra, S., Lodge, D. M., & Egan, S. P.
616 (2017). Environmental DNA (eDNA) detects the invasive crayfishes *Orconectes rusticus* and
617 *Pacifastacus leniusculus* in large lakes of North America. *Hydrobiologia*, 800, 173–185.
618 <https://doi.org/10.1007/s10750-017-3210-7>

619 Lins, D. M., de Marco Jr, P., Andrade, A. F., & Rocha, R. M. (2018). Predicting global ascidian
620 invasions. *Diversity and Distributions*, 24, 692–704. <https://doi.org/10.1111/ddi.12711>

621 Locke, A. (2009). A screening procedure for potential tunicate invaders of Atlantic Canada. *Aquatic*
622 *Invasions*, 4, 71–79. <https://doi.org/10.3391/ai.2009.4.1.7>

- 623 Locke, A., & Carman, M. (2009). In situ growth of the colonial ascidian *Didemnum vexillum* under
624 different environmental conditions. *Aquatic Invasions*, 4, 275–278.
625 <https://doi.org/10.3391/ai.2009.4.1.27>
- 626 Lyman, J. M., Good, S. A., Gouretski, V. V., Ishii, M., Johnson, G. C., Palmer, M. D., Smith, D. M.,
627 & Willis, J. K. (2010). Robust warming of the global upper ocean. *Nature*, 465, 334–337.
628 <https://doi.org/10.1038/nature09043>
- 629 Madariaga, D. J., Rivadeneira, M. M., Tala, F., & Thiel, M. (2014). Environmental tolerance of the
630 two invasive species *Ciona intestinalis* and *Codium fragile*: their invasion potential along a
631 temperate coast. *Biological Invasions*, 16, 2507–2527. [https://doi.org/10.1007/s10530-014-](https://doi.org/10.1007/s10530-014-0680-7)
632 [0680-7](https://doi.org/10.1007/s10530-014-0680-7)
- 633 Marins, F. O., Novaes, R. L., Rocha, R. M., & Junqueira, A. O. (2010). Non indigenous ascidians in
634 port and natural environments in a tropical Brazilian bay. *Zoologia*, 27, 213–221.
635 <http://dx.doi.org/10.1590/S1984-46702010000200009>
- 636 Molnar, J. L., Gamboa, R. L., Revenga, C., & Spalding, M. D. (2008). Assessing the global threat of
637 invasive species to marine biodiversity. *Frontiers in Ecology and the Environment*, 6, 485–492.
638 <https://doi.org/10.1890/070064>
- 639 Moraitis, M. L., Tsikopoulou, I., Geropoulos, A., Dimitriou, P. D., Papageorgiou, N., Giannoulaki,
640 M., Valavanis, V. D., Karakassis, I. (2018). Molluscan indicator species and their potential use in
641 ecological status assessment using species distribution modeling. *Marine Environmental*
642 *Research*, 140, 10–17. <https://doi.org/10.1016/j.marenvres.2018.05.020>
- 643 Nagar, L. R., & Shenkar, N. (2016). Temperature and salinity sensitivity of the invasive ascidian
644 *Microcosmus exasperatus* Heller, 1878. *Aquatic Invasions*, 11, 33–43.
645 <http://dx.doi.org/10.3391/ai.2016.11.1.04>
- 646 NBN Atlas. (2019). NBN Atlas website at <http://www.nbnatlas.org>. Accessed 20 November 2019

647 Nydam, M. L., Giesbrecht, K. B., & Stephenson, E. E. (2017). Origin and dispersal history of two
648 colonial ascidian clades in the *Botryllus schlosseri* species complex. *PloS ONE*, 12, e0169944.
649 <https://doi.org/10.1371/journal.pone.0169944>

650 Nydam, M. L., & Harrison, R. G. (2007). Genealogical relationships within and among shallow-
651 water *Ciona* species (Asciacea). *Marine Biology*, 151, 1839–1847.
652 <https://doi.org/10.1007/s00227-007-0617-0>

653 OBIS. (2019). Ocean Biogeographic Information System. Intergovernmental Oceanographic
654 Commission of UNESCO. www.iobis.org. Accessed from R via robis ([https://CRAN.R-](https://CRAN.R-project.org/package=robis)
655 [project.org/package=robis](https://CRAN.R-project.org/package=robis)) on 2019-11-20

656 Olenin, S., Elliott, M., Bysveen, I., Culverhouse, P. F., Daunys, D., Dubelaar, G. B. J., Gollasch, S.,
657 Gouletquer, P., Jelmert, A., Kantor, Y., Mézeth, K. B., Minchin, D., Occhipint-Ambrogi, A.,
658 Olenina, I., Vandekerkhove, J. (2011). Recommendations on methods for the detection and
659 control of biological pollution in marine coastal waters. *Marine Pollution Bulletin*, 62, 2598–
660 2604. <https://doi.org/10.1016/j.marpolbul.2011.08.011>

661 Pérez-Portela, R., Arranz, V., Rius, M., & Turon, X. (2013). Cryptic speciation or global spread? The
662 case of a cosmopolitan marine invertebrate with limited dispersal capabilities. *Scientific Reports*,
663 3, 3197. <https://doi.org/10.1038/srep03197>

664 Perry, A. L., Low, P. J., Ellis, J. R., & Reynolds, J. D. (2005). Climate change and distribution shifts
665 in marine fishes. *Science*, 308, 1912–1915. <https://doi.org/10.1126/science.1111322>

666 Pineda, M. C., López-Legentil, S., & Turon, X. (2011). The whereabouts of an ancient wanderer:
667 global phylogeography of the solitary ascidian *Styela plicata*. *PLoS ONE*, 6, e25495.
668 <https://doi.org/10.1371/journal.pone.0025495>

669 Pineda, M. C., McQuaid, C. D., Turon, X., López-Legentil, S., Ordóñez, V., & Rius, M. (2012).
670 Tough adults, frail babies: an analysis of stress sensitivity across early life-history stages of

671 widely introduced marine invertebrates. *PLoS ONE*, 7, e46672.
672 <https://doi.org/10.1371/journal.pone.0046672>

673 Pimentel, D., Zuniga, R., & Morrison, D. (2005). Update on the environmental and economic costs
674 associated with alien-invasive species in the United States. *Ecological Economics*, 52, 273–288.
675 <https://doi.org/10.1016/j.ecolecon.2004.10.002>

676 Potts, W. M., Henriques, R., Santos, C. V., Munnik, K., Anson, I., Dufois, F., Booth, A. J.,
677 Kirchner, C., Sauer, W. H., & Shaw, P. W. (2014). Ocean warming, a rapid distributional shift,
678 and the hybridization of a coastal fish species. *Global Change Biology*, 20, 2765–2777.
679 <https://doi.org/10.1111/gcb.12612>

680 R Core Team. (2017). R: A language and environment for statistical computing. R Foundation for
681 Statistical Computing, Vienna, Austria.

682 Raitzos, D. E., Beaugrand, G., Georgopoulos, D., Zenetos, A., Pancucci-Papadopoulou, A. M.,
683 Theocharis, A., & Papathanassiou, E. (2010). Global climate change amplifies the entry of
684 tropical species into the Eastern Mediterranean Sea. *Limnology and Oceanography*, 55, 1478–
685 1484. <https://doi.org/10.4319/lo.2010.55.4.1478>

686 Rhein, M., Rintoul, S. R., Aoki, S., Campos, E., Chambers, D., Feely, R. A., Gulev, S., Johnson, G.
687 C., Josey, S.A., Kostianoy, A., Mauritzen, C., Roemmich, D., Talley, L.D., & Wang, F. (2014).
688 Observations: Ocean. In: *Climate Change 2013: The Physical Science Basis. Contribution of*
689 *Working Group I to the Fifth Assessment Report of the Intergovernmental Panel on Climate*
690 *Change* [Stocker, T.F., Qin, D., Plattner, G. K., Tignor, M., Allen, S. K., Boschung, J., Nauels,
691 A., Xia, Y., Bex, V., & Midgley, P. M. (eds.)]. Cambridge University Press, Cambridge, United
692 Kingdom and New York, NY, USA.

693 Rius, M., Clusella-Trullas, S., McQuaid, C. D., Navarro, R. A., Griffiths, C. L., Matthee, C. A.,
694 Heyden, S., & Turon, X. (2014). Range expansions across ecoregions: interactions of climate

695 change, physiology and genetic diversity. *Global Ecology and Biogeography*, 23, 76–88.
696 <https://doi.org/10.1111/geb.12105>

697 Rius, M., Turon, X., Ordóñez, V., & Pascual, M. (2012). Tracking invasion histories in the sea: facing
698 complex scenarios using multilocus data. *PLoS ONE*, 7, e35815.
699 <https://doi.org/10.1371/journal.pone.0035815>

700 Sambrook, K., Holt, R. H., Sharp, R., Griffith, K., Roche, R. C., Newstead, R. G., ... & Jenkins, S. R.
701 (2014). Capacity, capability and cross-border challenges associated with marine eradication
702 programmes in Europe: The attempted eradication of an invasive non-native ascidian,
703 *Didemnum vexillum* in Wales, United Kingdom. *Marine Policy*, 48, 51–58.
704 <https://doi.org/10.1016/j.marpol.2014.03.018>

705 Scheele, B. C., Pasmans, F., Skerratt, L. F., Berger, L., Martel, A., Beukema, W., ... & Canessa, S.
706 (2019). Amphibian fungal panzootic causes catastrophic and ongoing loss of biodiversity.
707 *Science*, 363, 1459–1463. <https://doi.org/10.1126/science.aav0379>

708 Shenkar, N., & Swalla, B. J. (2011). Global diversity of Ascidiacea. *PLoS ONE*, 6, e20657.
709 <https://doi.org/10.1371/journal.pone.0020657>

710 Simberloff, D., Martin, J. L., Genovesi, P., Maris, V., Wardle, D. A., Aronson, J., Courchamp, F.,
711 Galil, B., Garcia-Berthou, E., Pascal, M., Pyšek, P., Sousa, R., Tabacchi, E., Vilà, M. (2013).
712 Impacts of biological invasions: what's what and the way forward. *Trends in Ecology and*
713 *Evolution*, 28, 58–66. <https://doi.org/10.1016/j.tree.2012.07.013>

714 Simpson, T. J., Dias, P. J., Snow, M., Muñoz, J., & Berry, T. (2017). Real-time PCR detection of
715 *Didemnum perlucidum* (Monniot, 1983) and *Didemnum vexillum* (Kott, 2002) in an applied
716 routine marine biosecurity context. *Molecular Ecology Resources*, 17, 443–453.
717 <https://doi.org/10.1111/1755-0998.12581>

718 Sorte, C. J., Williams, S. L., & Zerebecki, R. A. (2010). Ocean warming increases threat of invasive

719 species in a marine fouling community. *Ecology*, 91, 2198–2204. <https://doi.org/10.1890/10->
720 0238.1

721 Stachowicz, J. J., Terwin, J. R., Whitlatch, R. B., & Osman, R. W. (2002). Linking climate change
722 and biological invasions: ocean warming facilitates nonindigenous species invasions.
723 *Proceedings of the National Academy of Sciences*, 99, 15497–15500.
724 <https://doi.org/10.1073/pnas.242437499>

725 Stefaniak, L., Lambert, G., Gittenberger, A., Zhang, H., Lin, S., & Whitlatch, R. B. (2009). Genetic
726 conspecificity of the worldwide populations of *Didemnum vexillum* Kott, 2002. *Aquatic*
727 *Invasions*, 4, 29–44. <https://doi.org/10.3391/ai.2009.4.1.3>

728 Swets, J. A. (1988). Measuring the accuracy of diagnostic systems. *Science*, 240, 1285–1293.
729 <https://doi.org/10.1126/science.3287615>

730 Syfert, M. M., Smith, M. J., & Coomes, D. A. (2013). The effects of sampling bias and model
731 complexity on the predictive performance of MaxEnt species distribution models. *PloS ONE*, 8,
732 e55158. <https://doi.org/10.1371/journal.pone.0055158>

733 Teske, P. R., Rius, M., McQuaid, C. D., Styan, C. A., Piggott, M. P., Benhissoune, S., ... & Cooke, G.
734 M. (2011). “Nested” cryptic diversity in a widespread marine ecosystem engineer: a challenge
735 for detecting biological invasions. *BMC Evolutionary Biology*, 11, 176.
736 <https://doi.org/10.1186/1471-2148-11-176>

737 Thiyagarajan, V., & Qian, P. Y. (2003). Effect of temperature, salinity and delayed attachment on
738 development of the solitary ascidian *Styela plicata* (Lesueur). *Journal of Experimental Marine*
739 *Biology and Ecology*, 290, 133–146. [https://doi.org/10.1016/S0022-0981\(03\)00071-6](https://doi.org/10.1016/S0022-0981(03)00071-6)

740 Thuiller, W., Georges, D., & Engler, R. (2014). biomod2: ensemble platform for species distribution
741 modeling. R package version 3.3.7.

742 Thuiller, W., Guéguen, M., Renaud, J., Karger, D. N., & Zimmermann, N. E. (2019). Uncertainty in

743 ensembles of global biodiversity scenarios. *Nature Communications*, 10, 1446.
744 <https://doi.org/10.1038/s41467-019-09519-w>

745 Tracy, B. M., Larson, K. J., Ashton, G. V., Lambert, G., Chang, A. L., & Ruiz, G. M. (2017).
746 Northward range expansion of three non-native ascidians on the west coast of North America.
747 *BioInvasions Record*, 6, 203–209. <https://doi.org/10.3391/bir.2017.6.3.04>

748 U.S. Geological Survey. (2019). Biodiversity Information Serving Our Nation (BISON). Available
749 at: <https://bison.usgs.gov>. Accessed 20 November 2019

750 VanDerWal, J., Shoo, L. P., Graham, C., & Williams, S. E. (2009). Selecting pseudo-absence data for
751 presence-only distribution modeling: how far should you stray from what you know? *Ecological*
752 *Modelling*, 220, 589–594. <https://doi.org/10.1016/j.ecolmodel.2008.11.010>

753 Van Zuiden, T. M., Chen, M. M., Stefanoff, S., Lopez, L., & Sharma, S. (2016). Projected impacts of
754 climate change on three freshwater fishes and potential novel competitive interactions. *Diversity*
755 *and Distributions*, 22, 603–614. <https://doi.org/10.1111/ddi.12422>

756 Vergés, A., Doropoulos, C., Malcolm, H. A., Skye, M., Garcia-Pizá, M., Marzinelli, E. M., Campbell,
757 A. H., Ballesteros, E., Hoey, A. S., Vila-Concejo, A., Bozec, Y., & Steinberg, P. D. (2016).
758 Long-term empirical evidence of ocean warming leading to tropicalization of fish communities,
759 increased herbivory, and loss of kelp. *Proceedings of the National Academy of Sciences*, 113,
760 13791–13796. <https://doi.org/10.1073/pnas.1610725113>

761 Vermeij, G.J., & and Roopnarine, P.D. (2008). The coming arctic invasion. *Science*, 321, 780–781.
762 <https://doi.org/10.1126/science.1160852>

763 Zhan, A., Briski, E., Bock, D. G., Ghabooli, S., & MacIsaac, H. J. (2015). Ascidians as models for
764 studying invasion success. *Marine Biology*, 162, 2449–2470. [https://doi.org/10.1007/s00227-](https://doi.org/10.1007/s00227-015-2734-5)
765 [015-2734-5](https://doi.org/10.1007/s00227-015-2734-5)

766 Zhan, A., Darling, J. A., Bock, D. G., Lacoursiere-Roussel, A., MacIsaac, H. J., & Cristescu, M. E.

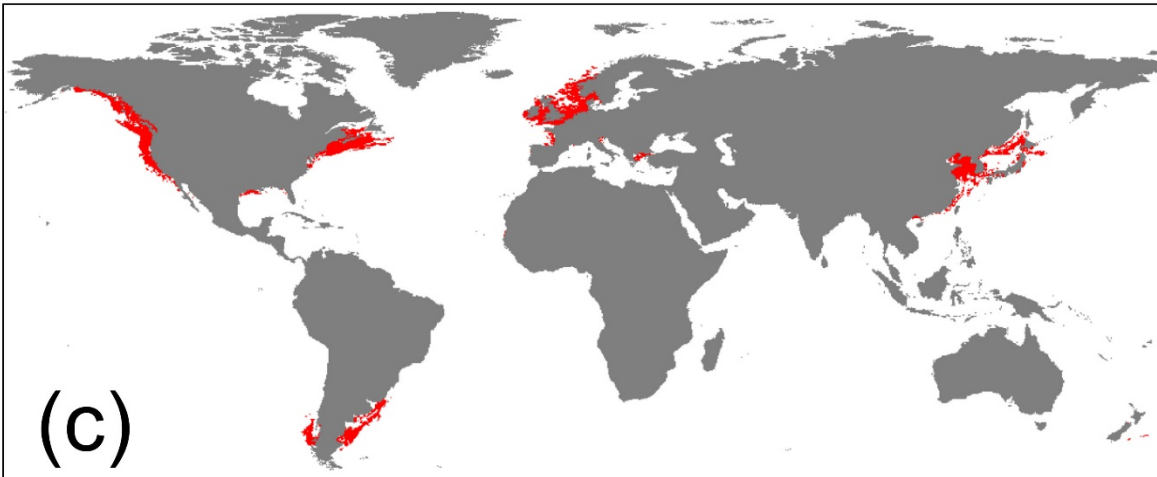
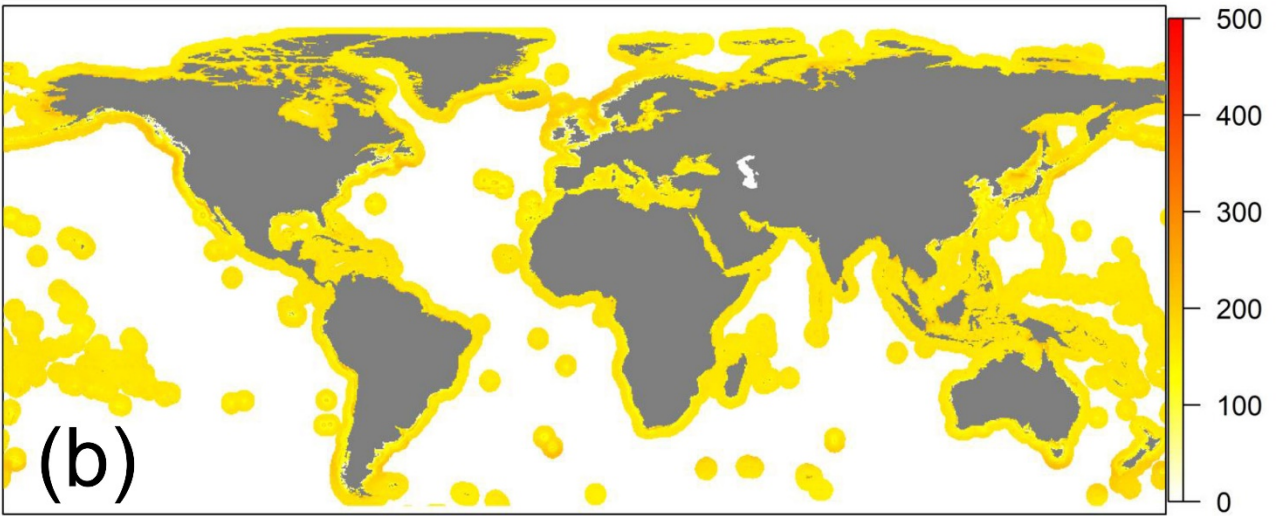
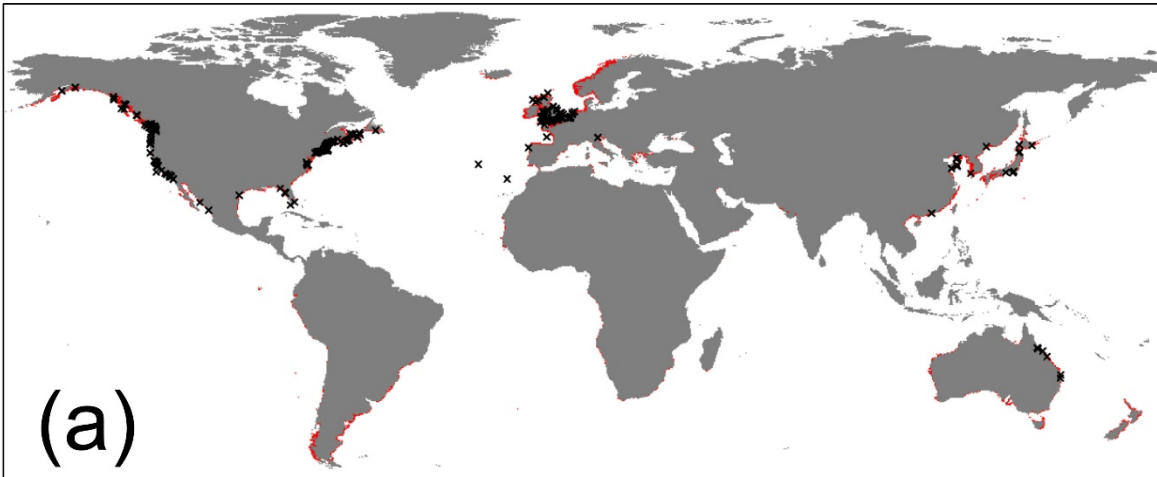
767 (2012). Complex genetic patterns in closely related colonizing invasive species. *Ecology and*
768 *Evolution*, 2, 1331–1346. <https://doi.org/10.1002/ece3.258>

Declaration of interests

The authors declare that they have no known competing financial interests or personal relationships that could have appeared to influence the work reported in this paper.

The authors declare the following financial interests/personal relationships which may be considered as potential competing interests:

1 Supporting Information



3 **Figure S1. Habitat suitability of *Botrylloides violaceus* under present-day climate conditions.**

4 Habitat suitability ranges from 0 to 1000. Black crosses indicate occurrence records of *B. violaceus*
5 used to develop species distribution models. 341 occurrence records of *B. violaceus* were used.

6 **Figure S1. (a) Suitable range of *Botrylloides violaceus* under present-day climate conditions**

7 **projected by ensemble SDM. Red area represents suitable range. Black crosses indicate occurrence**
8 **records of *B. violaceus* used to develop SDMs. 333 occurrence records of *B. violaceus* were used.**

9 **(b) Coefficient of variation of present-day species occurrence probability predicted by seven single**

10 **SDMs. Coefficient of variation in suitable range (i.e. red area in panel (a)) (45.863 ± 0.148) was**

11 **significantly lower than that in unsuitable range (163.505 ± 0.012) (Mann–Whitney *U* Test; $p <$**

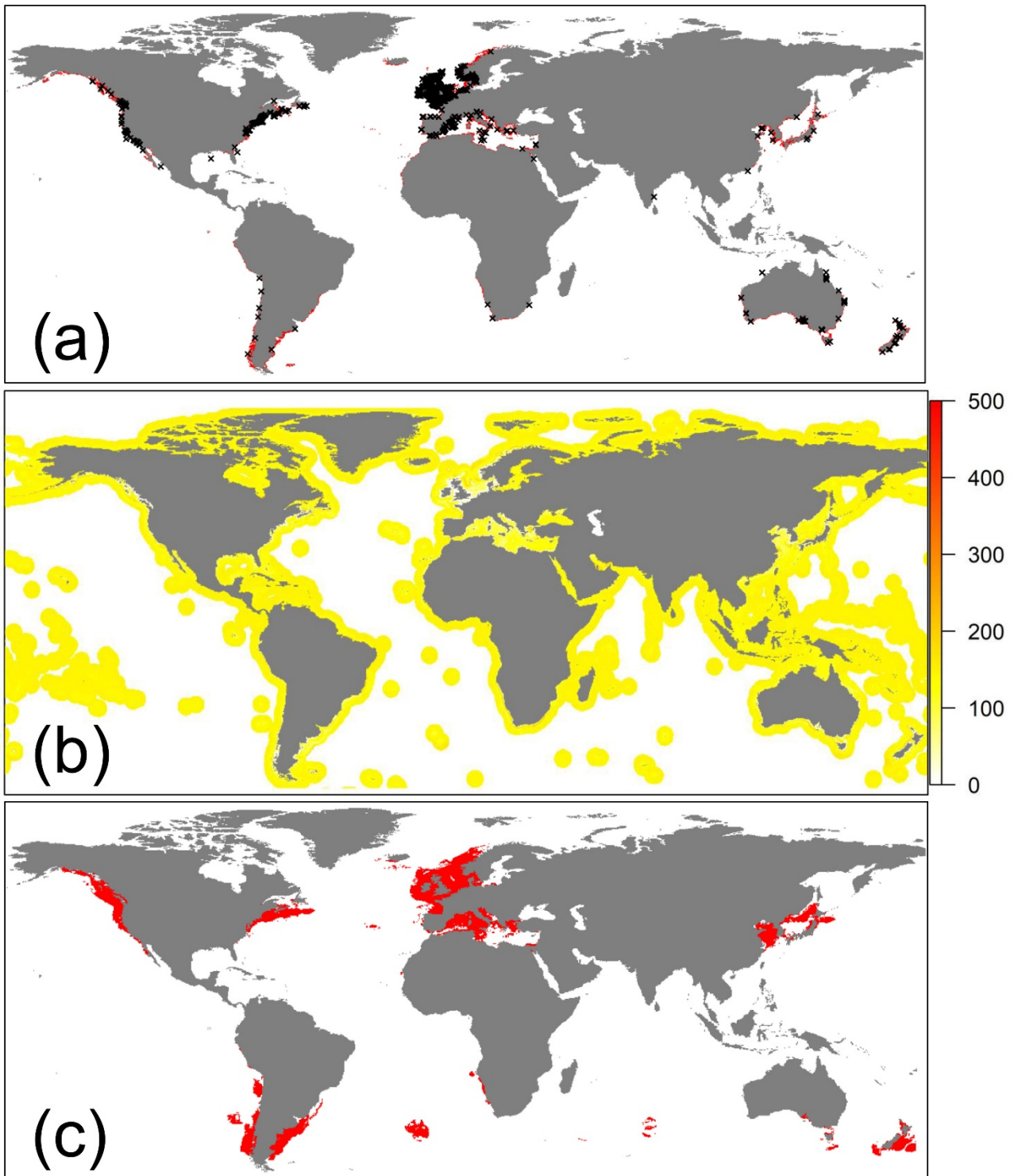
12 **2.2×10^{-16}). Results were expressed as mean \pm standard error. Coefficient of variation was calculated**

13 **as follows: coefficient of variation = standard deviation/mean*100%. (c) Suitable range of *B.***

14 ***violaceus* under present-day climate conditions projected by ensemble SDM without considering**

15 **water depth and distance to shore.**

16

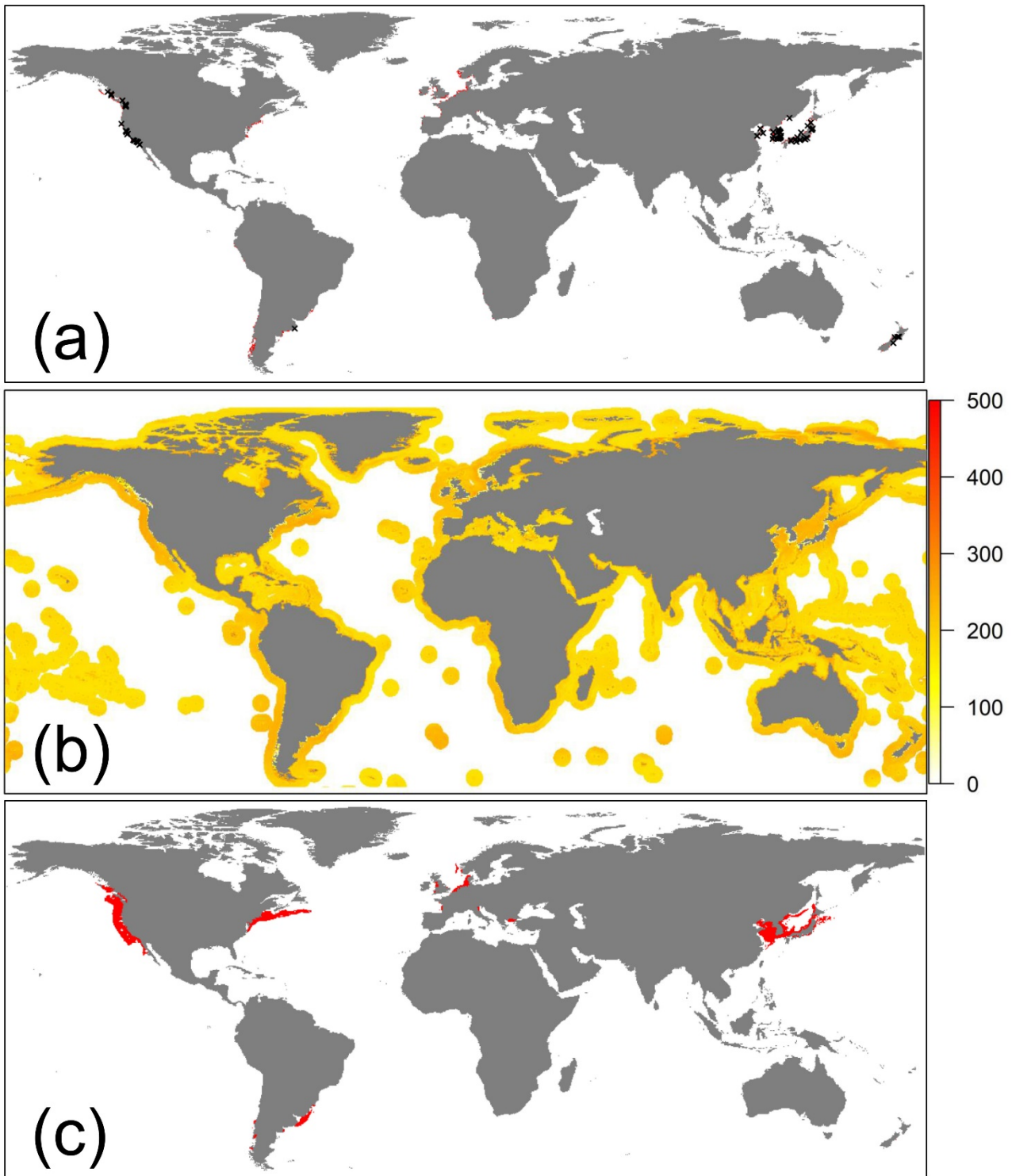


17

18 **Figure S2.** (a) Suitable range of *Botryllus schlosseri* under present-day climate conditions projected
 19 by ensemble SDM. Red area represents suitable range. Black crosses indicate occurrence records of
 20 *B. schlosseri* used to develop SDMs. 1367 occurrence records of *B. schlosseri* were used. (b)
 21 Coefficient of variation of present-day species occurrence probability predicted by seven single

22 SDMs. Coefficient of variation in suitable range (i.e. red area in panel (a)) (35.885 ± 0.113) was
23 significantly lower than that in unsuitable range (136.869 ± 0.010) (Mann–Whitney U Test; $p <$
24 2.2×10^{-16}). Results were expressed as mean \pm standard error. Coefficient of variation was calculated
25 as follows: coefficient of variation = standard deviation/mean*100%. (c) Suitable range of *B.*
26 *schlosseri* under present-day climate conditions projected by ensemble SDM without considering
27 water depth and distance to shore.

28

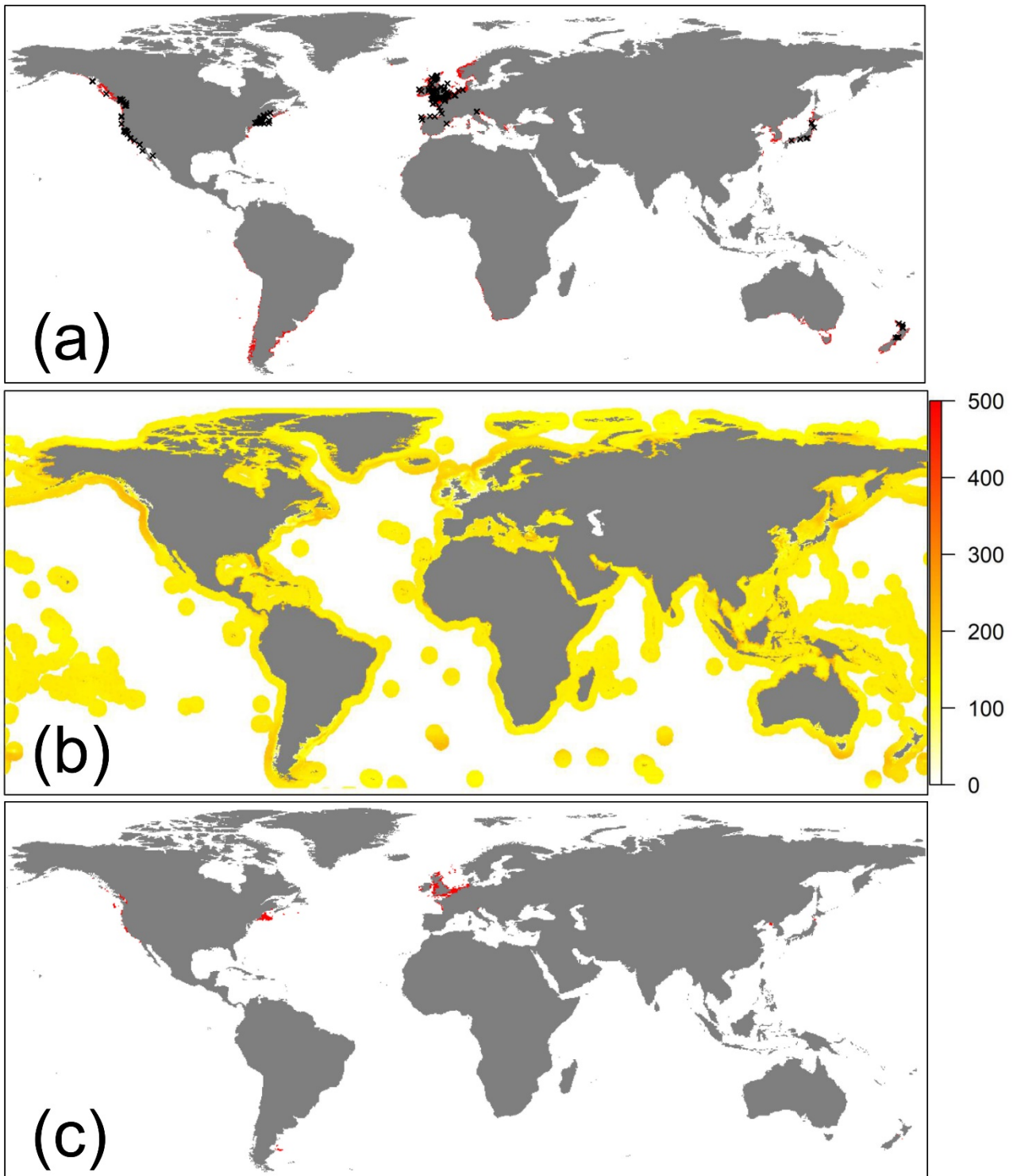


29

30 **Figure S3.** (a) Suitable range of *Ciona savignyi* under present-day climate conditions projected by
 31 ensemble SDM. Red area represents suitable range. Black crosses indicate occurrence records of *C.*
 32 *savignyi* used to develop SDMs. 93 occurrence records of *C. savignyi* were used. (b) Coefficient of
 33 variation of present-day species occurrence probability predicted by seven single SDMs. Coefficient

34 of variation in suitable range (i.e. red area in panel (a)) (33.827 ± 0.223) was significantly lower
35 than that in unsuitable range (194.589 ± 0.019) (Mann–Whitney U Test; $p < 2.2 \times 10^{-16}$). Results
36 were expressed as mean \pm standard error. Coefficient of variation was calculated as follows:
37 coefficient of variation = standard deviation/mean*100%. (c) Suitable range of *C. savignyi* under
38 present-day climate conditions projected by ensemble SDM without considering water depth and
39 distance to shore.

40

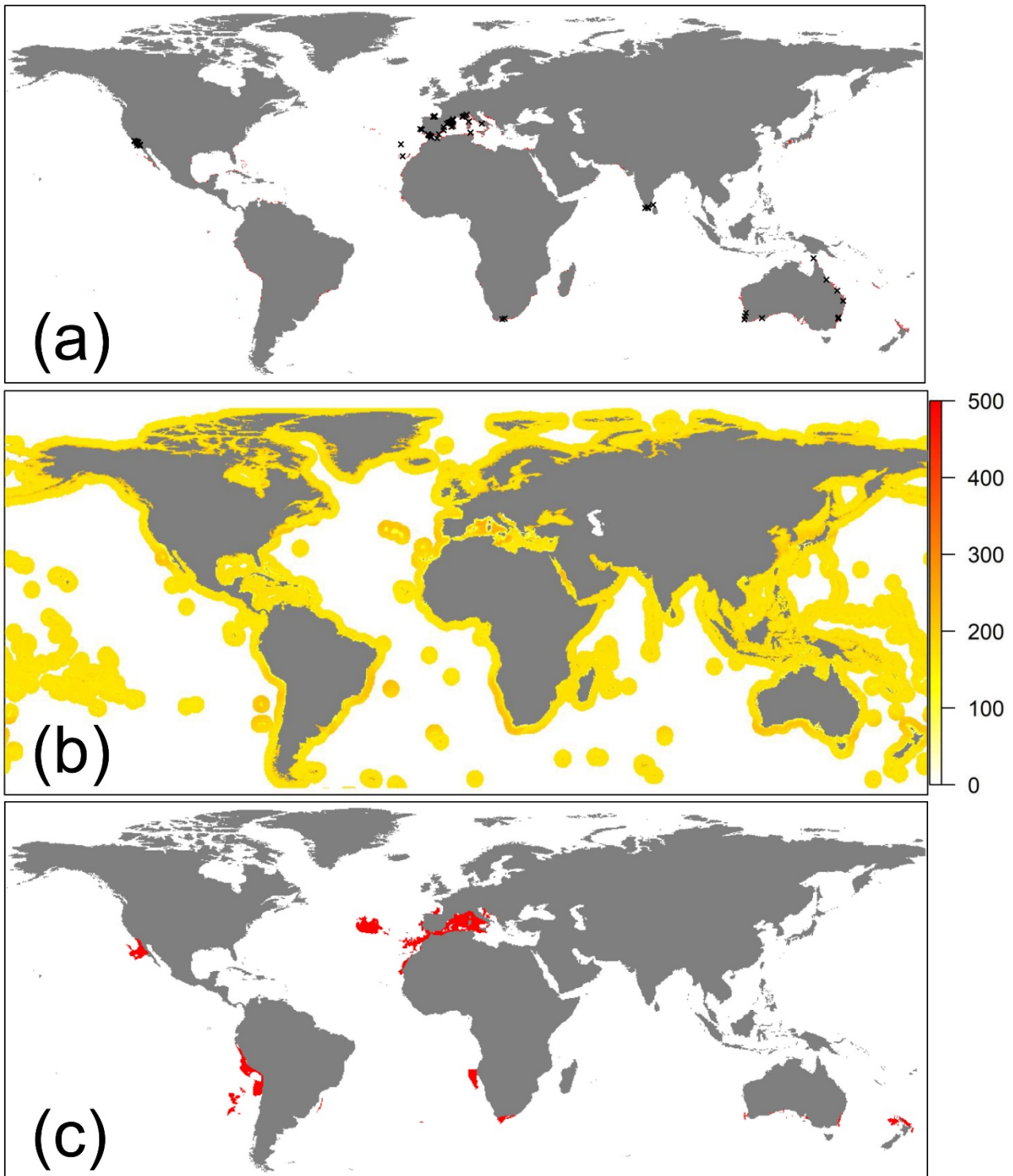


41

42 **Figure S4.** (a) Suitable range of *Didemnum vexillum* under present-day climate conditions projected
 43 by ensemble SDM. Red area represents suitable range. Black crosses indicate occurrence records of
 44 *D. vexillum* used to develop SDMs. 252 occurrence records of *D. vexillum* were used. (b)
 45 Coefficient of variation of present-day species occurrence probability predicted by seven single

46 SDMs. Coefficient of variation in suitable range (i.e. red area in panel (a)) (46.178 ± 0.157) was
47 significantly lower than that in unsuitable range (156.493 ± 0.016) (Mann–Whitney U Test; $p <$
48 2.2×10^{-16}). Results were expressed as mean \pm standard error. Coefficient of variation was calculated
49 as follows: coefficient of variation = standard deviation/mean*100%. (c) Suitable range of *D.*
50 *vexillum* under present-day climate conditions projected by ensemble SDM without considering
51 water depth and distance to shore.

52

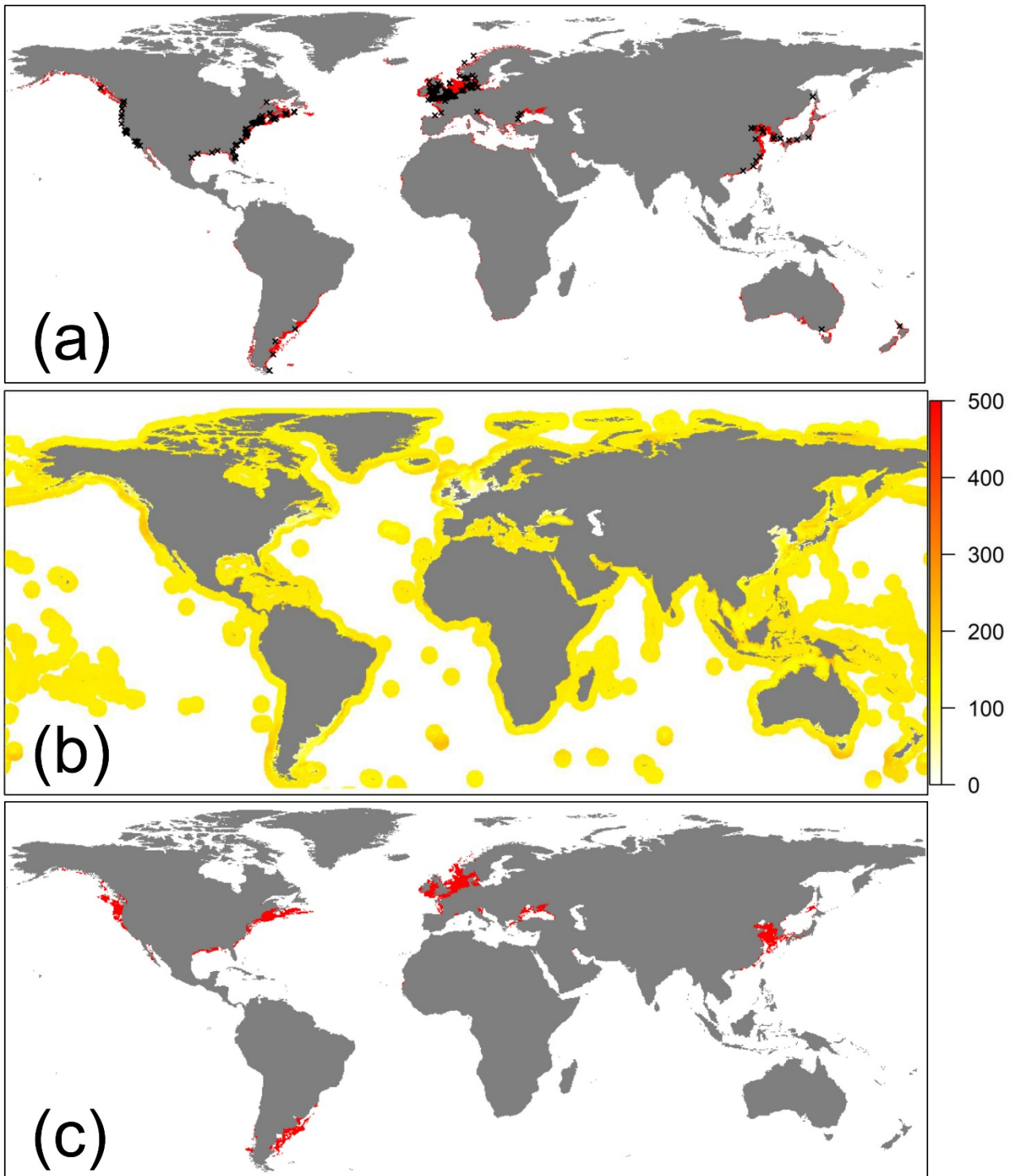


53

54 **Figure S5.** (a) Suitable range of *Microcosmus squamiger* under present-day climate conditions
 55 projected by ensemble SDM. Red area represents suitable range. Black crosses indicate occurrence
 56 records of *M. squamiger* used to develop SDMs. 77 occurrence records of *M. squamiger* were used.
 57 (b) Coefficient of variation of present-day species occurrence probability predicted by seven single

58 SDMs. Coefficient of variation in suitable range (i.e. red area in panel (a)) (31.695 ± 0.220) was
59 significantly lower than that in unsuitable range (171.412 ± 0.013) (Mann–Whitney U Test; $p <$
60 2.2×10^{-16}). Results were expressed as mean \pm standard error. Coefficient of variation was calculated
61 as follows: coefficient of variation = standard deviation/mean*100%. (c) Suitable range of *M.*
62 *squamiger* under present-day climate conditions projected by ensemble SDM without considering
63 water depth and distance to shore.

64

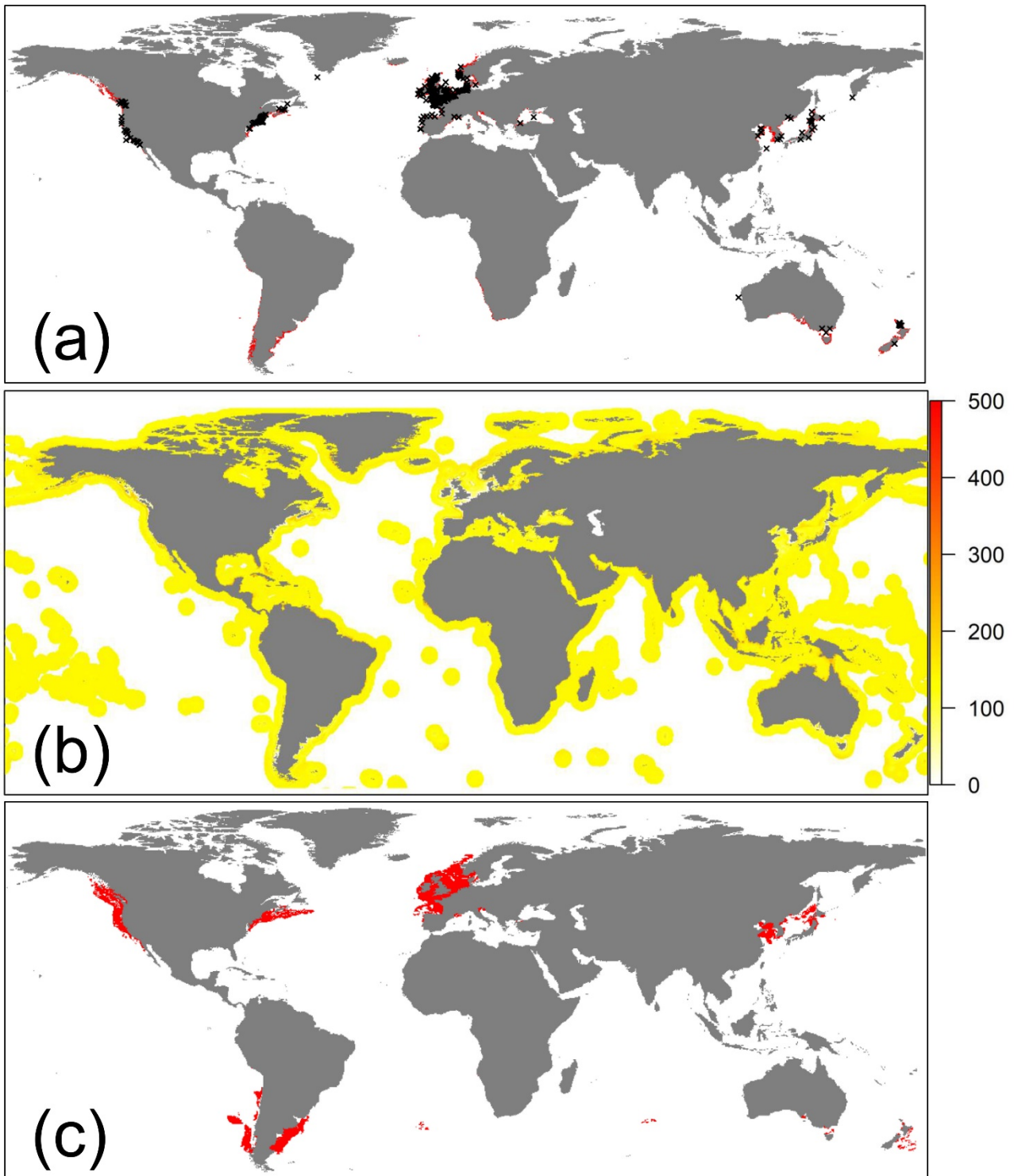


65

66 **Figure S6.** (a) Suitable range of *Molgula manhattensis* under present-day climate conditions
 67 projected by ensemble SDM. Red area represents suitable range. Black crosses indicate occurrence
 68 records of *M. manhattensis* used to develop SDMs. 368 occurrence records of *M. manhattensis*
 69 were used. (b) Coefficient of variation of present-day species occurrence probability predicted by

70 seven single SDMs. Coefficient of variation in suitable range (i.e. red area in panel (a)) ($51.039 \pm$
71 0.108) was significantly lower than that in unsuitable range (154.883 ± 0.012) (Mann–Whitney U
72 Test; $p < 2.2 \times 10^{-16}$). Results were expressed as mean \pm standard error. Coefficient of variation was
73 calculated as follows: coefficient of variation = standard deviation/mean*100%. (c) Suitable range
74 of *M. manhattensis* under present-day climate conditions projected by ensemble SDM without
75 considering water depth and distance to shore.

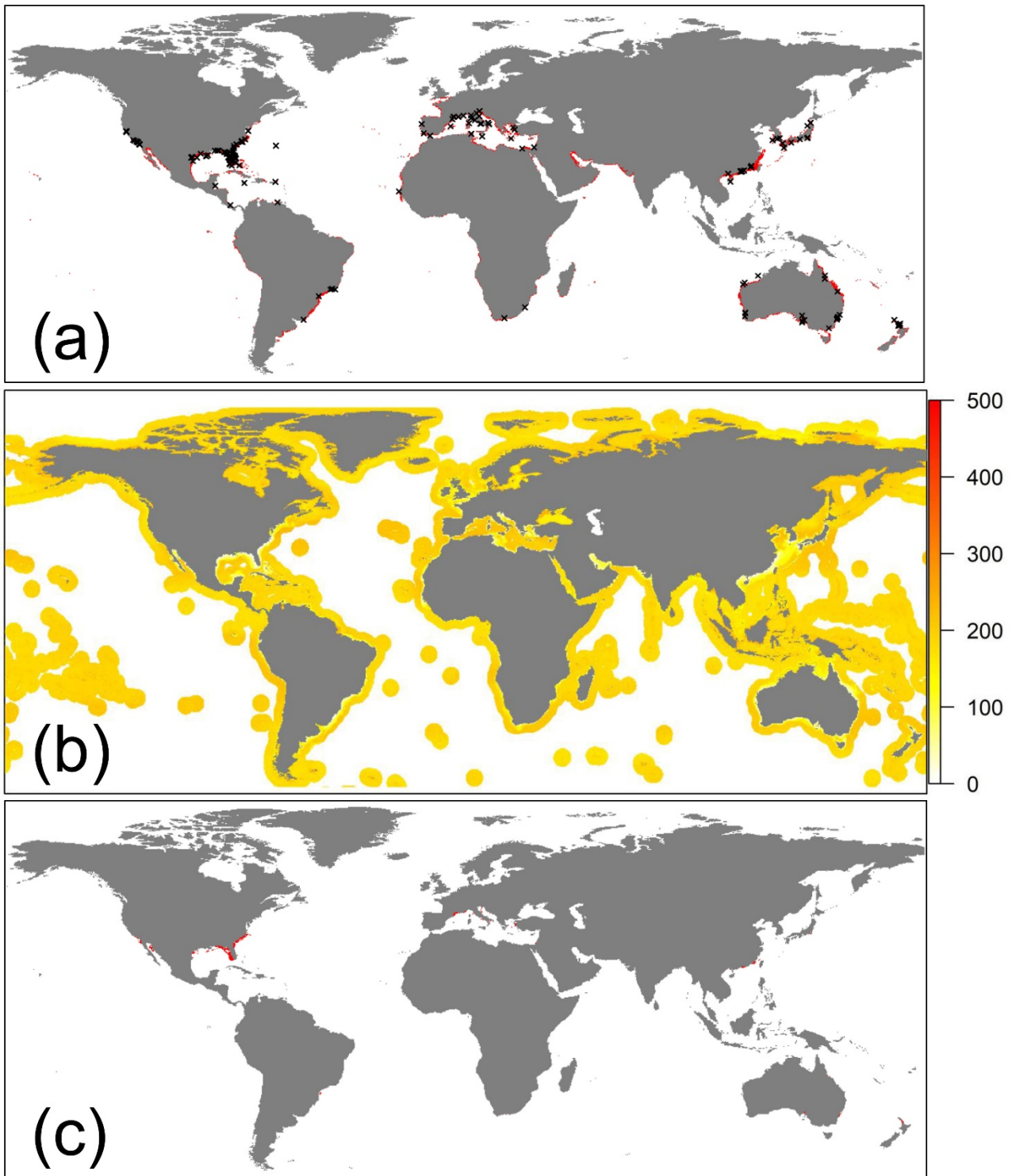
76



77

78 **Figure S7.** (a) Suitable range of *Styela clava* under present-day climate conditions projected by
 79 ensemble SDM. Red area represents suitable range. Black crosses indicate occurrence records of *S.*
 80 *clava* used to develop SDMs. 521 occurrence records of *S. clava* were used. (b) Coefficient of
 81 variation of present-day species occurrence probability predicted by seven single SDMs. Coefficient

82 of variation in suitable range (i.e. red area in panel (a)) (37.301 ± 0.169) was significantly lower
83 than that in unsuitable range (137.427 ± 0.010) (Mann–Whitney U Test; $p < 2.2 \times 10^{-16}$). Results
84 were expressed as mean \pm standard error. Coefficient of variation was calculated as follows:
85 coefficient of variation = standard deviation/mean*100%. (c) Suitable range of *S. clava* under
86 present-day climate conditions projected by ensemble SDM without considering water depth and
87 distance to shore.
88



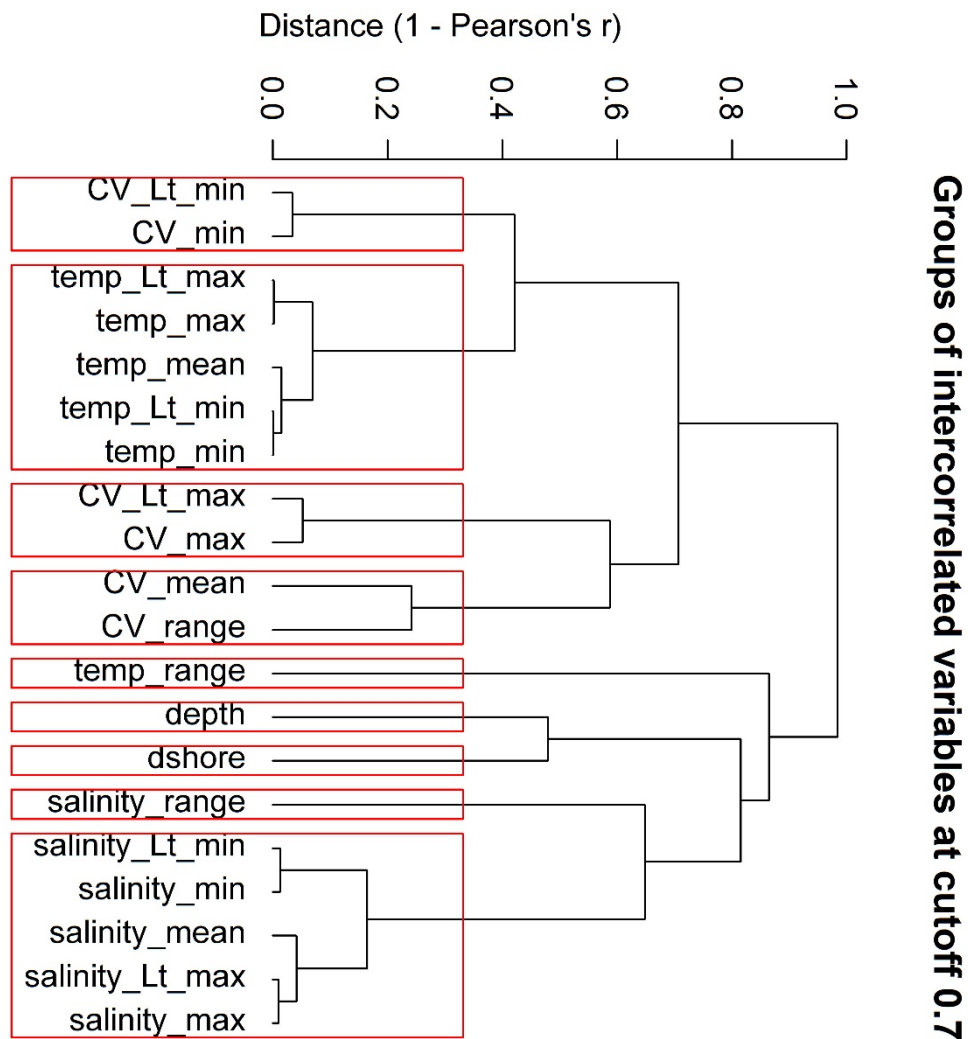
89

90 **Figure S8.** (a) Suitable range of *Styela plicata* under present-day climate conditions projected by
 91 ensemble SDM. Red area represents suitable range. Black crosses indicate occurrence records of *S.*
 92 *plicata* used to develop SDMs. 178 occurrence records of *S. plicata* were used. (b) Coefficient of
 93 variation of present-day species occurrence probability predicted by seven single SDMs. Coefficient

94 of variation in suitable range (i.e. red area in panel (a)) (39.872 ± 0.101) was significantly lower
95 than that in unsuitable range (184.213 ± 0.016) (Mann–Whitney U Test; $p < 2.2 \times 10^{-16}$). Results
96 were expressed as mean \pm standard error. Coefficient of variation was calculated as follows:
97 coefficient of variation = standard deviation/mean*100%. (c) Suitable range of *S. plicata* under
98 present-day climate conditions projected by ensemble SDM without considering water depth and
99 distance to shore.

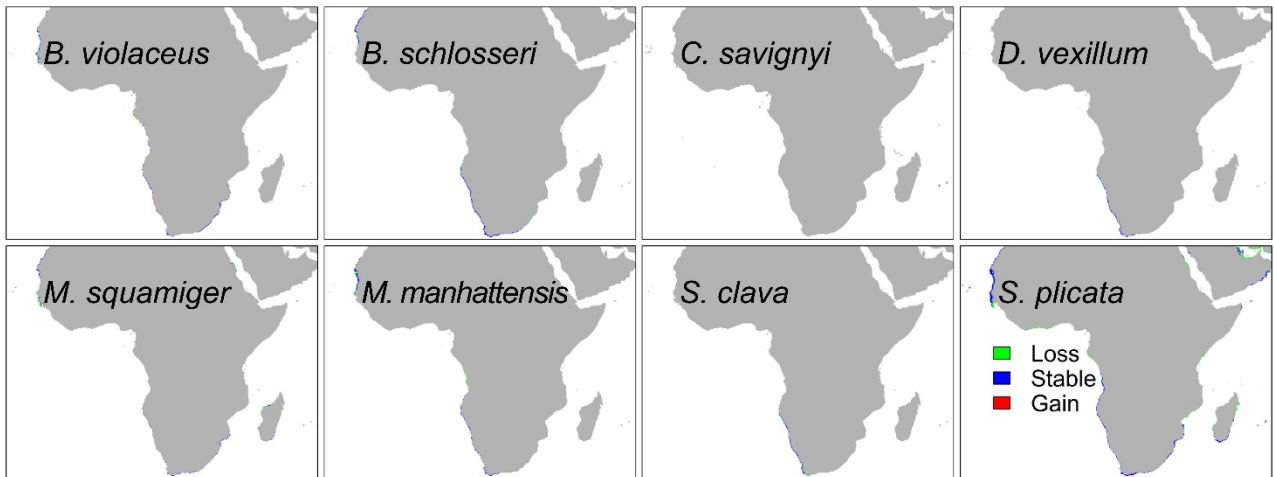
100

101



102

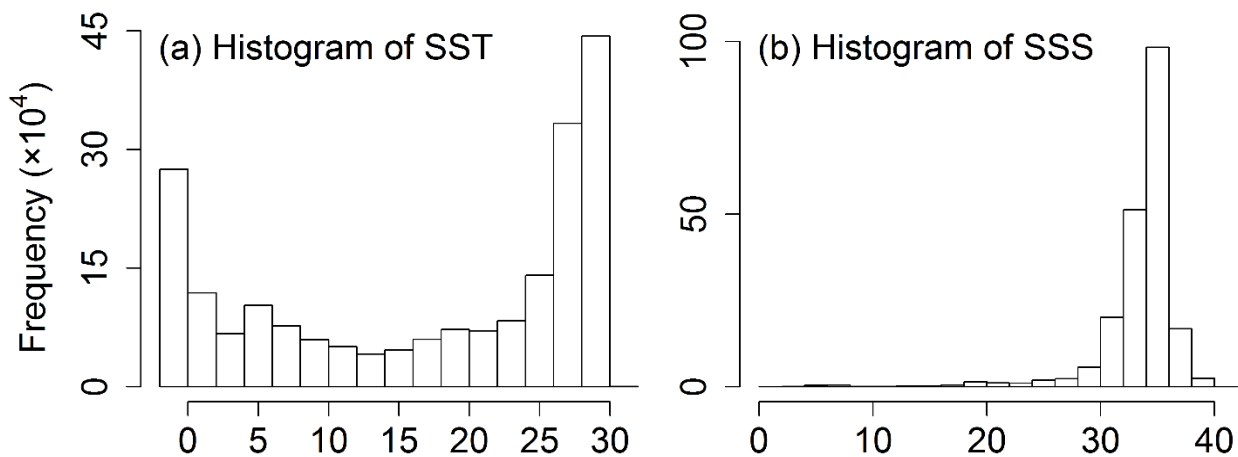
103 **Figure S9.** Collinearity analysis results of the twentyeight marine predictor variables. temp: **annual**
 104 sea surface temperature; Lt: mean values of the minimum and maximum records per year; CV:
 105 current velocity. depth: water depth; dshore: distance to the shore. Detailed descriptions about
 106 predictors can be found in Bio-ORACLE v2.0 (<http://www.bio-oracle.org>). Only one predictor was
 107 selected among highly correlated predictors (i.e., Pearson's correlation coefficients $|r| > 0.7$).



109

110 **Figure S10.** Predicted range shifts of the eight ascidians along African coastal areas in 2050s under
 111 RCP45 scenario. RCP: representative concentration pathway. 2050s: 2040-2050. Stable areas (in
 112 blue) indicate habitats that are predicted to be suitable under both present-day and future climates;
 113 loss areas (in green) show areas which are predicted no longer to be suitable in future; gain areas (in
 114 red) represent habitats that are predicted to be suitable in future.

115



116

117 **Figure S11.** Frequency histograms of (a) mean sea surface temperature (SST) (in °C) and (b) mean
 118 sea surface salinity (SSS) (in ‰) within the Exclusive Economic Zone (i.e., within 370 km of the
 119 coast). SST is evenly distributed while SSS mainly concentrates between 30 to 38‰.

120 **Table S1** Mean (\pm standard error) AUC values of the ten algorithms used to predict habitat suitability of eight ascidians. AUC: area under the receiver
 121 operating characteristic curve. AUC values were calculated by a five-fold cross-validation with 10 repetitions. The numbers in red represent algorithms
 122 with AUC < 0.90. ANN: artificial neural network, CTA: classification tree analysis, FDA: flexible discriminant analysis, GAM: generalized additive
 123 model, GBM: generalized boosting model, GLM: generalized linear model, MARS: multiple adaptive regression splines, Maxent: maximum entropy,
 124 RF: random forest, SRE: surface range envelop.

Species	ANN	CTA	FDA	GAM	GBM	GLM	MARS	Maxent	RF	SRE
<i>Botrylloides violaceus</i>	0.979 (\pm 0.003)	0.951 (\pm 0.008)	0.979 (\pm 0.003)	0.975 (\pm 0.003)	0.991 (\pm 0.001)	0.991 (\pm 0.001)	0.990 (\pm 0.002)	0.916 (\pm 0.006)	0.989 (\pm 0.002)	0.845 (\pm 0.010)
<i>Botryllus schlosseri</i>	0.984 (\pm 0.002)	0.970 (\pm 0.002)	0.982 (\pm 0.002)	0.988 (\pm 0.002)	0.991 (\pm 0.001)	0.988 (\pm 0.001)	0.990 (\pm 0.001)	0.945 (\pm 0.005)	0.993 (\pm 0.001)	0.868 (\pm 0.006)
<i>Ciona savignyi</i>	0.989 (\pm 0.005)	0.951 (\pm 0.011)	0.991 (\pm 0.001)	0.925 (\pm 0.018)	0.996 (\pm 0.003)	0.980 (\pm 0.006)	0.984 (\pm 0.008)	0.893 (\pm 0.015)	0.998 (\pm 0.000)	0.786 (\pm 0.013)
<i>Didemnum vexillum</i>	0.983 (\pm 0.002)	0.964 (\pm 0.007)	0.984 (\pm 0.002)	0.971 (\pm 0.005)	0.994 (\pm 0.001)	0.991 (\pm 0.002)	0.991 (\pm 0.002)	0.922 (\pm 0.008)	0.990 (\pm 0.002)	0.843 (\pm 0.011)
<i>Microcosmus squamiger</i>	0.952 (\pm 0.010)	0.919 (\pm 0.018)	0.983 (\pm 0.001)	0.899 (\pm 0.015)	0.991 (\pm 0.001)	0.977 (\pm 0.006)	0.970 (\pm 0.008)	0.931 (\pm 0.014)	0.968 (\pm 0.008)	0.778 (\pm 0.024)
<i>Molgula manhattensis</i>	0.982	0.955	0.981	0.983	0.994	0.987	0.992	0.925	0.994	0.832

	(± 0.002)	(± 0.006)	(± 0.002)	(± 0.002)	(± 0.001)	(± 0.002)	(± 0.001)	(± 0.008)	(± 0.001)	(± 0.012)
<i>Styela clava</i>	0.982	0.966	0.988	0.986	0.993	0.993	0.994	0.950	0.992	0.866
	(± 0.004)	(± 0.005)	(± 0.001)	(± 0.002)	(± 0.001)	(± 0.001)	(± 0.001)	(± 0.004)	(± 0.001)	(± 0.005)
<i>Styela plicata</i>	0.977	0.931	0.977	0.959	0.991	0.985	0.984	0.952	0.992	0.810
	(± 0.005)	(± 0.013)	(± 0.003)	(± 0.008)	(± 0.001)	(± 0.002)	(± 0.003)	(± 0.012)	(± 0.001)	(± 0.009)

127 **Table S2** Mean (\pm standard error) TSS values of the ten algorithms used to predict habitat suitability of eight ascidians. TSS: true skill statistics. TSS
 128 values were calculated by a five-fold cross-validation with 10 repetitions. The numbers in red represent algorithms with TSS < 0.75. ANN: artificial
 129 neural network, CTA: classification tree analysis, FDA: flexible discriminant analysis, GAM: generalized additive model, GBM: generalized boosting
 130 model, GLM: generalized linear model, MARS: multiple adaptive regression splines, Maxent: maximum entropy, RF: random forest, SRE: surface
 131 range envelop.

Species	ANN	CTA	FDA	GAM	GBM	GLM	MARS	Maxent	RF	SRE
<i>Botrylloides violaceus</i>	0.926 (\pm 0.009)	0.914 (\pm 0.013)	0.880 (\pm 0.010)	0.928 (\pm 0.005)	0.947 (\pm 0.005)	0.932 (\pm 0.003)	0.936 (\pm 0.007)	0.829 (\pm 0.012)	0.939 (\pm 0.006)	0.690 (\pm 0.019)
<i>Botryllus schlosseri</i>	0.935 (\pm 0.003)	0.922 (\pm 0.004)	0.910 (\pm 0.005)	0.932 (\pm 0.004)	0.941 (\pm 0.003)	0.928 (\pm 0.004)	0.938 (\pm 0.003)	0.880 (\pm 0.010)	0.943 (\pm 0.002)	0.736 (\pm 0.012)
<i>Ciona savignyi</i>	0.963 (\pm 0.010)	0.927 (\pm 0.017)	0.968 (\pm 0.005)	0.850 (\pm 0.036)	0.985 (\pm 0.006)	0.957 (\pm 0.011)	0.959 (\pm 0.016)	0.786 (\pm 0.030)	0.990 (\pm 0.001)	0.572 (\pm 0.025)
<i>Didemnum vexillum</i>	0.924 (\pm 0.009)	0.934 (\pm 0.011)	0.897 (\pm 0.009)	0.924 (\pm 0.009)	0.948 (\pm 0.008)	0.956 (\pm 0.005)	0.958 (\pm 0.004)	0.843 (\pm 0.017)	0.944 (\pm 0.009)	0.685 (\pm 0.022)
<i>Microcosmus squamiger</i>	0.872 (\pm 0.027)	0.843 (\pm 0.032)	0.912 (\pm 0.008)	0.792 (\pm 0.028)	0.920 (\pm 0.017)	0.920 (\pm 0.018)	0.902 (\pm 0.016)	0.844 (\pm 0.024)	0.879 (\pm 0.017)	0.555 (\pm 0.048)
<i>Molgula manhattensis</i>	0.929	0.910	0.891	0.928	0.939	0.927	0.934	0.843	0.942	0.664

	(± 0.008)	(± 0.008)	(± 0.006)	(± 0.006)	(± 0.004)	(± 0.004)	(± 0.005)	(± 0.015)	(± 0.007)	(± 0.025)
<i>Styela clava</i>	0.934	0.938	0.908	0.943	0.956	0.949	0.955	0.896	0.951	0.733
	(± 0.009)	(± 0.005)	(± 0.007)	(± 0.005)	(± 0.004)	(± 0.004)	(± 0.003)	(± 0.008)	(± 0.004)	(± 0.010)
<i>Styela plicata</i>	0.898	0.875	0.894	0.891	0.940	0.926	0.938	0.881	0.928	0.621
	(± 0.009)	(± 0.014)	(± 0.010)	(± 0.013)	(± 0.009)	(± 0.006)	(± 0.010)	(± 0.022)	(± 0.010)	(± 0.017)
